A MORPHOLOGICAL AND BIOCHEMICAL STUDY ON THE HEMISECTED RAT SPINAL CORD IMPLANTED WITH CULTURED ASTROCYTES

BY

JOIE JIE WANG

A THESIS SUBMITTED IN PARTIAL FULFILMENT OF THE REQUIREMENTS FOR THE DEGREE OF

MASTER OF PHILOSOPHY

DIVISION OF BASIC MEDICAL SCIENCES
GRADUATE SCHOOL
THE CHINESE UNIVERSITY OF HONG KONG

JUNE 1993

ABSTRACT

One of the objectives of the present study was to investigate the histological response of the hemisected adult rat spinal cord in the presence or absence of cultured astrocytes. Morphological and biochemical methods were applied to assess whether implanted astrocytes could exert an effect on neurite growth. Adult Sprague-Dawley rats were anesthetised with Nembutal (50 mg/kg) and the spinal cords were hemisected at the L_3 level. Astrocytes (95-98% purity) were obtained from neonatal rat cortex and introduced into the lesioned spinal cord either in suspension injection (HA group) or cultured on gelfoam (HAG) first. The control groups were rats which had hemisection with injection of culture media (HH) or with gelfoam grafted alone (HG).

At different time points after surgery (2 weeks to 2 months) the spinal cord was removed and processed for routine light and electron microscopy, gel electrophoresis, immunoblotting and immunofluorescence staining. Decreased GFAP immunostaining and volume of scar tissue over time were found in all groups indicating that the spinal cord underwent gradual recovery. However, as early as two weeks, and thereafter, a significantly smaller volume of scar tissue was consistently found in the experimental groups. This is also reflected in the immunoblotting which showed decreased amount of GFAP in the experimental group.

Ultrastructural observations of the area around the lesion 2 months after surgery showed that the experimental group had

more neurites and synapses, agreeing with the observations on the immunostaining for NF and also the immunoblotting. However, PHAL labelling of the implanted astrocytes showed that they migrated at a rate of 0.6 mm/day from the original implanted site. The results therefore suggested that the cultured astrocytes probably exerted their effect over a short time period (less than 2 weeks) around the lesion site. They could have altered the microenvironment and as a consequence less scar tissue was formed. Hence, there was less barrier to the regrowth of nerve fibres.

ACKNOWLEDGEMENTS

I am very much indebted to Dr. M.I. Chuah, my supervisor, Department of Anatomy, for her patient guidance, valuable advice and help at every aspect throughout my study. For all these, I would like to express my deepest gratitude to her.

I am pleased to have this opportunity to acknowledge my appreciation to Prof. J.A. Gosling for providing facilities and for encouraging academic interaction among research students; to Prof. P.C. Leung, Department of Orthopaedics and Traumatology, C.U.H.K., for his valuable advice and guidance on the present study; to Dr. M.C. Yu, Department of Anatomy, Cell Biology and Injury Sciences, New Jersey Medical School, for his enthusiastic help and support.

My thanks are also due to members of the Department of Anatomy, C.U.H.K., particularly to Ms. C. Au, Ms. J. Hou, Ms. J. Kung and Mr. S. Wong, for their professional advice and technical assistance.

Finally, I am grateful to my parents and my friends, for their limitless concern and support throughout this study.

TABLE OF CONTENTS

LIST OF TABLE

LIST OF FIGURES

LIST OF ABBREVIATIONS

Ara-C Cytosine arabinoside.

BSA Bovine serum albumin.

CNS Central nervous system.

CST Corticospinal tract.

DMEM Dulbecco's Modified Eagle's Medium.

DSC Dorsal spinocerebellar tract.

FITC Fluorescein isothiocyanate.

GFAP Glial fibrillary acidic protein.

HA Hemisection with cultured astrocyte suspension injected at the time of lesion.

HAG Hemisection with immediate implantation of astrocytes cultured on gelfoam.

H & E Hemotoxylin and Eosin staining.

HBSS Hank's Balanced Salt Solution.

HG Hemisection with gelfoam implantation alone.

HH Hemisection with injection of HBSS only.

MEM-H Minimum Essential Medium Eagle-HEPES.

MW Molecular weight.

N-CAM Neural cell adhesion molecule.

NF Neurofilament.

NGF Nerve growth factor.

NY Nuclear yellow.

PB Phosphate buffer.

PF Paraformaldehyde.

PHAL Phaseolus vulgaris leucoagglutinin.

PLL Poly-L-lysine.

PNS Peripheral nervous system.

RST Rubrospinal tract.

RT Room temperature.

SC Spinal cord.

SEM Scanning electron microscopy.

TB True blue.

TEM Transmission electron microscopy

TRITC Tetramethylrhodamine isothiocyanate.

TTBS Tween 20 in Tris-buffered saline.

VSC Ventral spinocerebellar tract.

I. Introduction

I.1. Fibre tracts of the rat spinal cord

The spinal cord (SC) plays an important role in conducting impulses between the brain and the peripheral nervous system.

The gray matter of the SC contains a large number of neurons and their dendrites in addition to even larger number of neuroglial cells. However, the white matter consists mainly of myelinated axons. The pathways in the white matter are divided into ascending and descending groups. The positions of some important ascending and descending pathways are indicated below (Grant, 1985; Tracey, 1985):

The dorsal columns contain both sensory and motor pathways in rats (Fig.1). The former are the tracts of the gracilis and cuneatus fasciculus. The latter is the fibres of the corticospinal tract (CST). In rats, the majority of crossed fibres in the CST is limited in the ventral most portion of the dorsal column of the SC, after decussating in the caudal medulla. These axons descend and terminate in the dorsomedial part of the dorsal horn at all levels of the SC. The uncrossed CST is small but easily identifiable in ventral SC in the rat cervical region. More caudally the tract becomes less distinct.

In lateral part of the SC, two of the sensory pathways are the dorsal and ventral spinocerebellar tracts (DSC and VSC). The motor pathway is the rubrospinal tract (RST), which projects its axons in the dorsolateral fasciculus of the SC. The tract terminates in the

ventrolateral aspect of the dorsal horn and intermediate portion of the ventral horn throughout the entire length of the SC.

In the ventral white matter of the SC, the cells of origin of spinothalamic tract are generally located in the dorsal horn, and their axons cross within a few segments to ascend directly to the thalamus.

If hemisection is performed in the SC, all the sensory and motor tracts mentioned above will be severed.

I.2. Histopathological responses to spinal cord injuries

The common type of SC damage may be the result of penetrating trauma by knives, deafferentation or excitotoxic injuries (Bovolenta et al., 1991). These injuries most often produce a variable degree of laceration or contusion. More seriously, they cause transection of the SC with necrosis in the involved segments. Neuronal atrophy and necrosis may appear from 12 hours to several weeks after axotomy in the SC (Barr and Hamilton, 1948; Barron and Doolin, 1969; Lieberman, 1971 and 1974; Grafstein, 1975).

Wallerian degeneraion was described in 1850 by Waller, A.V., who noted that when nerve axons were severed, the portion distal to the section became fragmented (Robertson and Dinsdale, 1972). This phenomenon can be observed with axotomy either in PNS or CNS. Following physical trauma, macrophages from intact or disrupted vessels migrate to the injury site in response to the influence of chemotactic stimuli. The macrophages form about 15% of the proliferating cells at two weeks post-lesion (Adrian et al.,

1978). The axonal fragments are subsequently digested by macrophages and the degenerating myelin sheath is transformed into a chain of lipid droplets. Following necrosis and removal of cell debris, cystic cavities are created in a region 2 mm rostral and caudal to the lesion site (Robertson and Dinsdale, 1972).

Several studies report that the most common proliferating cells following transection of the SC or optic nerve are the microglia (Adrian and William, 1973; Adrian et al., 1978; Privat et al., 1981). In the transected SC at two weeks post-lesion, the microglia form 50% of the dividing cells.

At the same time that microglia and macrophages are proliferating at the lesion site, a fibroglial scar begins to form (Lampert and Cressman, 1964; Mattews et al., 1979; Feringa et al., 1980; Guth et al., 1980). Astrocytes proliferate resulting in dense aggregates of astrocytic processes which contain large amounts of glial fibrillary acidic protein (GFAP) (Lampert and Cressman, 1964; Feringa et al., 1980). The resulting astrocytic gliosis prevents regenerative outgrowth (Lieberman, 1974).

Besides the cellular events observed at the axonal lesion site, chromatolysis is seen in the cell body as early as two days post-lesion. The cell soma becomes swollen, the nucleus migrates to the periphery, and the nucleoli enlarge (Robertson and Dinsdale, 1972). Subsequently, the Nissl substance disintegrates and the perikaryon becomes highly eosinophilic. This abnormal morphology may persist for many months before neuronal death occurs (Cajal,

1928; Nathaniel and Nathaniel, 1973; Egan et al., 1977; Shamboul, 1979).

I.3. Failure of CNS regeneration

There are different stages during nerve regeneration in the PNS. After axons are severed, cell bodies undergo chromatolysis, and axons undergo Wallerian degeneration. Subsequently, the morphology of the cell body recovers, and vigorous sprouting of fibres occurs at the proximal stump. Schwann cells in the distal segment proliferate to form long cylindrical aggregates. Axons grow at the rate of about 1 mm per day until they reach muscle or a sensory location (Ramon and Cajal, 1928; Robertson and Dinsdale, 1972). The time period for recovery is dependent upon the length of axons that needs to be reconstituted.

As described in the earlier sections, lesions of central tracts either result in very limited axonal sprouting or slow atrophy and death of the affected neurons. Several possible explanations have been put forward to account for this failure in regeneration.

Intrinsic inability of CNS neurons themselves to regenerate

Clark (1942 and 1943) observed that axons of the CNS failed to grow into grafts of peripheral nerve and concluded that central neurons are incapable of regenerating their axons. Clemente (1964), however, found that neurites in the transected SC did sprout at first, but no complete synapse reconstruction of the nerve tissue was established. Cajal (1928) found that the proximal

stumps of severed axons sprouted at first, but they degenerated about one month after the initial vigorous regrowth. Lampert and Cressman (1964) confirmed these findings after noting the same results in the thoracic SC of adult rats following total laminectomy. It appears then that central nerve fibres are capable of regrowing initially. Accordingly, specific environmental factors have been proposed to argue for the lack of axonal regrowth.

Inappropriate synapse without normal functioning

Bernstein and Bernstein (1969 and 1971) transected the SC of the goldfish and examined the ultrastructure 1 - 3 months post-surgery. These studies revealed that the regenerated central axons of the SC had grown out of their original tracts for only short distances. The fine tips of these axons had short terminal boutons that formed axo-axonic synapses with each other. The neurons appeared, at least in part, to be inhibiting their own growth by the inappropriate formation of synaptic junctional complexes.

Progressive necrosis and cystic cavities

Progressive necrosis and cystic cavity formation are often considered reasons for an abortive attempt at regeneration (Kao, 1974). Guth et al. (1981 and 1983) demonstrated that one way of minimising necrosis and cystic cavity formation was to use hibernating animals for SC lesion studies. In hibernating animals, numerous body functions including collagen synthesis and

immunological responses are depressed (Landau and Dawe, 1958; Lyman and O'Brien, 1960). Consequently, in their studies in which they transected the midthoracic SC of hibernating squirrels, minimal necrosis was obtained. The histological alteration in the SC showed loose accumulation of macrophages and little collagenous scarring in the lesion site. At the same time, they observed extensive regeneration of intrinsic SC and dorsal root fibres.

Autoimmune explanation for the failure of regeneration

It was suggested by Feringa et al. (1973), Berry and Riches (1974) that damage to the brain or the SC leads to the breakdown of the blood-brain barrier. Thereafter, the CNS autoantigens become exposed to the immune environment. The exposed antigens bind with humoral and cell-bound antibodies at the lesion area. It is possible that the resulting antibody-antigen complexes hinder the regeneration of axons in CNS. Unlike CNS, successful regeneration in PNS is due to rapid phagocytosis and denaturation of antigens by the Schwann cells surrounding the degenerated axons (Berry and Riches, 1974).

Glial scarring

Glial scar is formed as a result of hypertrophy and proliferation of astrocytes, particularly fibrous astrocytes adjacent to the lesion site (Latov et al., 1979). This has been verified by immunohistochemical and autoradiographic studies which demonstrated that uptake of radiolabelled thymidine was present in highly immunoreactive GFAP-positive fibrous astrocytes (Latov et

al., 1979). In studies involving hemisection of the SC, light microscopic observations suggested that the reactive astrocytic gliosis acted as a physical barrier to the regeneration of the lesioned SC axons (Chambers, 1955; Windle, 1956; Guth et al., 1981).

Absence of Schwann cells in the CNS

In the PNS, the arrangement of Schwann cells and their basement membranes provide a guiding structure for regenerating axons (Arteta 1956). Experiments which demonstrate that retinal ganglion cells can regenerate in peripheral nerve grafts indicate that Schwann cells play an important role in helping the nerve fibres to regrow (Anderson et al., 1983; Berry et al., 1988). Optic axonal regeneration through a freeze-dried sciatic nerve graft was delayed until the graft had been invaded by Schwann cells. Hence, the absence of Schwann cells in the CNS may be partly responsible for the lack of regeneration.

Schwann cells secrete substances such as laminin and nerve growth factors which are trophic to axonal growth after injury (Kiernan 1979). Laminin, one of the matrix glycoprotein, is secreted by immature and cultured astrocytes (Liesi et al., 1983). Components of the extracellular matrix have been implicated in the regulation of axonal growth. This indicated a role for laminin in the development of the CNS. Chiu et al. (1991) confirmed that laminin was a potent promotor of neurite outgrowth in cultures of both central and peripheral neurons.

Lack of requisite growth factors

Neurotrophic factors can stimulate axogenesis and facilitate the growth of the fibres to the target (Kiernan, 1978; Varon and Bunge, 1978). Berry (1979) suggested that nerve growth factors were absorbed by growing axons and conveyed to the perikaryon by retrograde transport where their actions on protein synsthesis were effected. Nerve growth factor (NGF) exerts a remarkable growth effect on developing sympathetic and sensory neurons and regenerating monoaminergic neurons (Bjerre et al., 1973). It has been shown that specific antiserum to NGF inhibits regeneration of monoaminergic neurons in the cortex (Bjerre et al., 1974) and also optic nerve fibre regeneration (Glaze and Turner, 1978). NGF-administered rats showed improved functional recovery of superior cervical ganglion neurons following axotomy (Hendry, 1975).

Other neurotrophic factors such as astroglial and fibroblast growth factors have been found to enhance the long-term survival in vitro of embryonic chick SC neurons including motoneurons (Unsicker et al., 1987). They also have mitogenic and differentiation -promoting effects on glial cells (Unsicker et al., 1987). In addition, FGF has been reported to enhance the regeneration of dopaminergic fibres in the striatum and to increase the survival of retinal ganglion cells after optic nerve lesion (Sievers et al., 1987; Baird and Walicke, 1989).

I.4. The use of transplants

Transplants of fetal nerve tissues

Fetal transplants show promise in the repair of brain injury. Transplants of fetal SC and cortex into adult rat SC generally survive better than transplants of other tissues, probably because the inherent capacity for cell division, growth and differentiation facilitate integration (Bernstein et al. 1984).

Reier (1985) pointed out that fetal SC implants formed a bridge for neurite growth by serving as a possible source of trophic stimuli. They may also establish appropriate neuronal relay circuits between the isolated stumps of the SC by replacing damaged intraspinal neurons. Reier et al. (1986) found that over 80% of the grafts of embryonic SC survived for 1-16 months in intraspinal cavities produced by partial lesion of both the neonatal and adult rat SC. Host nerve fibres were pre-labelled with wheat germ agglutinin-conjugated horseradish peroxidase (WGA-HRP) in order to trace their growth into the donor tissue. These embryonic SC transplants were observed to have the potential to restore some anatomical continuity between the isolated rostral and caudal stumps of the injured mammalian SC.

In Houle's study (1992), fetal tissue was transplanted after first removing the scar resulting from the hemisection of the SC. Growing fibres from the host were able to penetrate into the graft. The transplant also limited the extent to which a new scar was formed in response to a second injury to the SC.

However, another result may be obtained if the type of injury

and source of fetal tissue are different from what is described above. For example, Nornes et al. (1983) and Reier (1985) reported that transplants of embryonic brainstem into the denervated adult SC of rats acted as a source of neuron rather than a bridge or relay. The transplants were suspected to be partly responsible for some functional recovery - an enhancement of hindlimb flexion in adult rats.

Transplants of peripheral nerve tissues

Clemente (1964) considered that success in peripheral nerve regeneration resulted from the existence of some substances secreted from the Schwann cells. These factors possibly influenced the regrowth of CNS axons. When degenerated pieces of sciatic nerve were inserted into the cerebrum, extensive growth of central fibres into the graft after two weeks could be found (Clemente 1964).

More recently, experiments using neuroanatomical tracing methods have shown that the grafts of autologous peripheral nerve can promote the regrowth of some intraspinal fibres (Richardson et al., 1982).

Houle (1991) showed conclusively that axotomized neurons in the SC were able to regenerate if they were confronted with a peripheral nerve graft. In his experiment, he made several penetrating lesions with a sharpened tungsten wire in the rat lumbar SC. Next, true blue (TB) was introduced into the lesion site and it was taken up by the axotomized neurons. Seven days

later, a portion of the SC containing the glial scar was aspirated and segments of tibial nerve were sutured to the rostral and caudal stumps of the SC. Four weeks after, when nuclear yellow (NY) was introduced to the distal ends of the peripheral nerve graft, positive labelling was found in some neurons in the SC. These neurons were also labelled with TB indicating that these previously injured neurons had successfully regenerated into the peripheral nerve graft.

Transplants of neuroglial cells

With the advance of research techniques, it is now possible to obtain highly enriched populations of specific cell types. Hence, recent studies have explored the effects of implanting specific cells in CNS lesion sites.

Kuhlengel et al. (1990) reported the survival of purified Schwann cells following their implantation into the transected SC. The implanted Schwann cells consistently fasciculated the corticospinal tract fibres. In other experimental situations where the lesioned SC had been depleted of astrocytes and oligodendrocytes, it was found that implanted Schwann cells were able to myelinate demyelinated axons (Blakemore, 1983). In addition, implanted Schwann cells are also important in reducing central cavitation and astrocytic gliosis, thereby promoting axon growth (Martin et al., 1991).

Cultured astrocytes are another cell type whose growth promoting properties have been investigated in CNS lesion studies.

These glial cells have several advantages: they divide and grow well in tissue culture and are easy to obtain. They deliver growth factors that might prevent further neuronal degeneration after damage of CNS (Strecker, 1992).

Smith and Miller (1991) found that glial scar formation was suppressed by the transplantation of purified immature rat astrocytes into the adult forebrain. There was only a slight increase in anti-GFAP staining in the region of the implant. Axon outgrowth was enhanced at the same time. The grafted astrocytes were labelled with either fluorescent beads or BSA-conjugated colloidal gold to permit easy identification by light and electron microscopy.

Transplants of central neurons

Grafting of neurons into the adult CNS has provided a powerful vehicle for studying the survival and differentiation of these cells. Purified fetal noradrenergic locus coeruleus neurons were transplanted into the adult rat hippocampus from which the noradrenergic afferents had been removed by injection of bilateral 6-hydroxydopamine (6-OHDA). 4-8 months later, antibody against tyrosine hydroxylase or noradrenaline was used for immunohistochemistry. The noradrenergic axons were found to grow into and spread the host hippocampus from the implant. These fibres formed synaptic contacts with nonlabeled spines and shafts of dendrites in the host by EM. They received abundant host afferent input from nonlabeled axon terminals (Murata et al.,

1990).

Various methods have been successfully used to demonstrate the possibility of morpho-functional integration of grafted nervous tissue with host brain. Spontaneous and evoked activity of neurons in neocortical grafts were observed to be present. Integration of the transplant and host neuropil was shown.

I.5. Objectives of the present study

One of the objectives of this study is to compare the histological response of hemisected adult rat SC in the absence or presence of cultured neocortical astrocytes. Cultured astrocytes are introduced into the lesion site either as a cell suspension or as a pellet of gelfoam infiltrated by astrocytes. Following various periods of survival, light microscopic observations are made on the tissues and cells involved in the formation of reactive gliosis at the trauma region. The extent of scarring is measured in both the experimental and control groups.

Immunofluorescence methods are applied to identify the implanted astrocytes and also to demonstrate any resulting neurite growth. Electron microscopic observations are made to confirm the findings from the immunostaining.

The expression of various proteins in the lesioned SC in both the experimental and control groups is investigated by gel electrophoresis and Western blotting. The latter is directed at proteins specific for axonal regeneration. On completion of this project, one would have a better understanding of the influence

exerted by implanted neocortical astrocytes on regeneration.

II. Materials and Methods

II.1. Hemisection of rats

Three hundred and seventeen adult female Sprague-Dawley rats weighing about 300 grams were anesthetized with 2% Nembutal (50mg/kg) intraperitoneally. All the animals underwent laminectomy at the first lumbar vertebral level. The meninges of this area were stripped from the dorsal SC. The SC was hemisected on the right side at the third lumbar segment (corresponding to the first lumbar vertebral level) by a surgical scalpel blade (No.11). The median dorsal artery served as the landmark for the medial edge of the lesion (Fig 2 and 3).

Rats were divided into 4 groups.

1. Hemisection with cultured astrocyte suspension injected at the time of lesion (HA);

2. Hemisection with injection of Hank's Balanced Salt Solution (HBSS) (Sigma, St. Louis, U.S.A.) only (HH);

3. Hemisection with implantation of astrocytes cultured on gelfoam at the time of lesion (HAG);

4. Hemisection with gelfoam implantation alone (HG).

HA and HAG were the experimental group while HH and HG were the control.

Following surgical manipulation, size 4-0 surgical silk was used to suture muscles and adjoining skin. Rats were allowed to survive either 2 weeks, 1 month or 2 months.

II.2. Preparation of purified cortical astrocytes

This procedure was modified from the method of McCarthy and deVellis (1980). Poly-L-lysine (PLL) (Sigma) at a concentration of 5 ug/ml was coated on the bottom of Tissue Culture Flasks (T-75, Falcon, Becton Dickinson, New Jersey, U.S.A.) overnight. The following day, PLL was removed; the flasks were washed with sterile distilled water and dried for use.

New born (1-3 day old) Sprague-Dawley rat pups were decapitated, cerebral cortices were isolated and the meninges were stripped in Minimum Essential Medium Eagle-HEPES (MEM-H) (Sigma) under the dissection microscope. 0.125% trypsin (Gibco, New York, U.S.A.) in HBSS was used to dissociate the cells, which were incubated at 37^{o}C in water bath for 25 minutes. Trypsinization was stopped by trypsin inhibitor 12.5 ug/ml (Sigma) and deoxyribonuclease (DNAase) 10 ug/ml (Sigma). The tissue was then triturated with a fire polished Pasteur pipet. The suspension was filtered through a 72-um sterile nylon mesh, which eliminated large clumps of cells. The suspension was centrifuged at 1800 rpm for 10 minutes and the supernatant was removed. The cells were resuspended in the culture medium which was Dulbecco's Modified Eagle's Medium (DMEM) (Gibco) supplemented with 10% fetal Calf Serum (Gibco), 1% Penicillin Streptomycin (Sigma) and 1% MEM-Vitamin Solution (Gibco). This culture medium is thereafter referred to as CNS medium. Trypan blue of 0.1% concentration was used to determine the viability of cells under the microscope. The cells were seeded into T-75 flasks at a density of 1-2 x 10^{7}.

Usually, cortices from 4 animals yielded sufficient cells for culture into 3 flasks. The cells were cultured at an atmosphere of 5% CO_2 and 100% humidity.

During the first 10 days, neurons began to lift off from the more adherent astrocytes and ramained suspended in the medium. After 8-10 days, the adherent cells reached confluency and were ready for subculturing. The culture medium was changed and the cells were washed with DMEM 3 times. The cells were shaken on Lab-line Orbit Environ-shaker at 230 rpm at 37^{o}C overnight to remove the process-bearing top cells. The following day, the cells in the flasks were treated with 0.0125% trypsin. When the cells had contracted and begun to come off the bottom of the flasks, trypsinization was terminated by CNS. The cells from each flask were centrifuged at 1800 rpm for 10 minutes and were subcultured into 2 flasks at a concentration of 1 x 10^6 cells/flask. The cells were allowed to adhere for the next 24 hours and then treated with 10^{-7}M cytosine arabinoside (Ara-C) (Sigma) every 2 days thereafter for 1 week. After the last treatment of Ara-C, the medium was replaced with fresh CNS. At this point, a 95-98% pure astrocytes could be obtained at a density of 2.5 x 10^5 cells / flask.

To prepare a suspension for injection into the SC, astrocytes were treated with 0.006% trypsin and centrifuged. The resuspended cells were transferred to a pipet to be injected into the lesioned SC in 20 ul at 1.25 x 10^4 cells/ul. Approximately one third

would be lost during injection.

To prepare cultured astrocytes on gelfoam, pieces of gelfoam (3mm x 3mm x 2mm) were soaked in CNS medium, and dried on filter paper. Astrocytes were plated in a volume of 40 ul onto each piece of gelfoam at a concentration of 750 cells/ul. They were allowed to attach for 2 hours. After that, the culture medium, at a 1:1 composition of fresh CNS and medium conditioned by astrocytes was added. After 3 days' culture, the gelfoam with astrocytes was implanted into the lesioned SC.

II.3. Scanning electron microscopy

Scanning electron microscopy was conducted to investigate the survival of cultured astrocytes on gelfoam prior to implantaion into the hemisected spinal cord. The gelfoam infiltrated with cultured astrocytes was fixed with 2.5% glutaraldehyde in 0.1M PB at $4^{o}C$ for 30 minutes, and rinsed with 2 changes of distilled water for 10 minutes each. The gelfoam with astrocytes was then postfixed with 1% Osmium tetroxide (OsO_4) at room temperature for 1 hour, and washed with 2 changes of distilled water for 10 minutes each. The process of dehydration was through a sequential 10-minute wasing in graded alcohols from 50% to 100% followed by treatment in a mixture of 100% alcohol and Freon 113. The ratio of absolute alcohol and Freon 113 was 4:1, 3:2, 2:3, and 1:4 for 10 minutes each. After that, the cultured cells were dried with Freon 23 in critical point drier and coated with gold palladium. Specimens were viewed under the Jeol JSM-35CF SEM at 15 kV.

II.4. Histology--Light microscopy

Animals underwent anesthetization with 2% Nembutal (50 mg/kg) intraperitoneally. Cardiac perfusion was conducted with 0.9% saline followed by 10% buffered formalin. A 2.0-2.5 cm long segment of lumbar SC, including the lesioned area, was then taken out. The tissue was dehydrated in a tissue autoprocessor, containing an ascending series of ethanols, cleared in xylene and embedded in paraffin. Sections of 7 um thickness were made from the tissue, put on slides, and incubated in a 50^{o}C oven overnight. The following day, paraffin was removed with three 5-minute xylene washes. The sections were rehydrated in a graded series of ethanols followed by a rinse in tap water. After Hemotoxylin and Eosin (H & E) staining for 5 and 3 minutes respectively, sections were dehydrated in serial ethanols; and cleared again in xylene. Finally, they were mounted onto slides with Permount.

II.5. Measurement of volume of scar tissue

The volume of scar tissue at the lesioned site was measured by the following steps. From serial sections, the first one that had the lesion was saved. Fig.4 and 5 shows a typical longitudinal section taken from the SC. The dotted lines demarcate the boundary of the scar whose area was measured first by camera lucida drawing, followed by digitizing. The area of the scar on every 20th section was digitized. The total volume of scarring tissue was calculated by the following formula:

$$V = A \times 7 \times 20$$

V: total volume of scarring

A: total area of scarring derived by summing all the areas in each specimen.

7: thickness of sections

20: intervening sections

II.6. Immunofluorescence staining

Following a post-operative recovery period ranging from 2 weeks to 2 months, rats underwent anesthetization with 2% Nembutal and were perfused intracardially with 0.9% saline, followed by 4% paraformaldehyde(PF). A segment of the lumbar SC 2.0-2.5cm long, which included the lesion area, was removed and stored in 4% PF at $4^{o}C$ overnight.

Prior to sectioning, the segment of SC was frozen in liquid nitrogen and 10 um-thick longitudinal sections were cut on a cryomicrotome (Reichert-Jung 1800) at $-22^{o}C$. They were mounted on dry gelatin coated slides and allowed to dry.

Polyclonal rabbit anti-GFAP antibody (R anti-GFAP Ab, Sigma) (1:100) was used to stain for glial fibrillary acidic protein (GFAP). GFAP is an intermediate filament present in immature and mature astrocytes. Goat anti-rabbit immunoglubulin(IgG) antibody conjugated with fluorescein isothiocyanate (FITC) (Jackson) (1:100) was applied as a secondary antibody. Monoclonal mouse anti-neurofilament(NF) antibody (M anti-NF Ab, Sigma) (1:40) was used to label for the 200,000 dalton NF subunit which is expressed

in nerve fibres. FITC-conjugated goat antibody to mouse IgG (Jackson) (1:100) was the secondary antibody to M anti-NF Ab. Immunofluorescent staining for the neural cell adhesion molecule (N-CAM) was also performed. N-CAM is a glycoprotein membrane molecule commonly found in differentiating neurons and also cultured astrocytes (Chuong et al., 1984; Wong, 1991). It is believed to play a critical role in neuronal differentiation and tissue patterning during development (Edelman, 1985; 1988). Monoclonal mouse anti-NCAM antibody against all subunits (Sigma) (1:100) directed at all the subunits was used and the secondary antibody was either TRITC or FITC-conjugated goat anti mouse IgG (1:100).

Sections were fixed in 4% PF in moist chamber for 30 minutes, rinsed in 3 changes of 0.1 M phosphate buffer (PB), each of 5 minutes duration. Sections were blocked with 3% bovine serum albumin (BSA) (Sigma) for 1 hour at room temperature (RT) in humidified chamber. Primary antibodies were applied to the sections at 4^{o}C in a moist chamber overnight. Normal goat serum (NGS), acting as a blocking serum, was also applied in the same dilution. The following day, sections were rinsed in 0.1M PB 3 times in 1 hour at RT followed by secondary antibody labelling for 1 hour at RT. For double labelling, second primary and accompanying secondary antibodies were applied at this stage. Subsequently, sections were rinsed in 0.1M PB and mounted with mounting media, made up of 0.4 mg/ml of phenylenediamine in 0.1 M

sodium carbonate solution with 4 to 8 times volume of glycerol. Sections were observed in a fluorescence photomicroscope (Zeiss, West Germany).

Controls were stained under the same condition as the experimental ones except without primary antibodies.

Examination of the fate of grafted astrocytes

The plant lectin Phaseolus vulgaris leucoagglutinin (PHAL) conjugated with FITC (Sigma) was used to label the cultured astrocytes prior to transplantation. The astrocytes from each flask (2.0×10^5) were incubated at $37^{o}C$ for 4 hours by gentle agitation with PHAL-FITC (8 ug/ml). The percentage of labelled astrocytes was determined under the microscope. The astrocytes obtained from 1 flask were grafted into 1 animal and virtually 90% cells from one flask were labelled with PHAL-FITC (Fig.6).

At 1 week and 2 weeks post operation, animals were anesthetized with 2% Nembutal (50mg/kg) intraperitoneally, perfused with 0.9% saline, followed by 4% PF fixation. A segment of the lumbar SC 2.0-2.5 cm long, which contained the lesion site, was taken out and stored in 4% PF at $4^{o}C$ overnight. Longitudinal 10 um thick sections of the SC were made on the cryostat.

II.7. Transmission electron microscopy

Transmission electron microscopy (TEM) was conducted only in the groups with gelfoam implantation. Considerable healing of the lesioned SC tissue had normally occurred at 1 and 2 months post-operation, and the presence of the gelfoam was helpful in

demarcating the boundary of the lesioned area more clearly.

Animals were anesthetized with 2% Nembutal (50 mg/kg) intraperitoneally. Cardiac perfusion was conducted with 0.9% saline followed by 4% glutaraldehyde fixative. A piece of lumbar SC, 2.0-2.5 cm long, containing the lesioned area was taken out for fixation in 4% glutaraldehyde in 0.1M PB for 4 hours at RT. Fig.7 shows the location of the various blocks of SC obtained for TEM with respect to the lesion site. The intact contralateral half of the SC was discarded. A slight depression marking the lesion site could be observed. At the middle of the depression, a cut was made. At 2 mm above, another cut was made, and a block of the SC, designated block 2, was obtained. Blocks 1, 3 and 4 were obtained in the same way. Every block was 2 mm in length, which was optimal for TEM processing. Blocks 2 and 3 usually had gelfoam and they represented the lesion site. Block 1 was designated rostral part and block 4, the caudal.

These blocks were fixed with 4% glutaraldehyde in 0.1M PB for another 4 hours and then rinsed with PB 3 times, each of 5 minutes duration. They were then postfixed with 1% OsO_4 at RT for 1 hour followed by rinsing in distilled water. The process of dehydration was through a sequential 15-minute washing in graded ethanols from 70% to 100% followed by treatment in a mixture of 100% ethanol and Spurr. The ratio of absolute alcohol and Spurr was 2:1 for 1 hour, 1:1 for 2-4 hours and 1:2 for 1 hour or overnight. Then blocks were immersed in pure resin for 8 hours or overnight, after which,

they were embedded in 70°C oven for 16 hours in fresh Spurr.

The specimens were cut into ultrathin sections of thickness 80 nm by an ultramicrotome (Reichert-Jung) and mounted on copper grids of 200 mesh. The thin sections were stained with 1% saturated uranyl acetate solution for 15 minutes in the dark. They were washed in 50% methanol, dried on filter paper and stained with aqueous lead citrate for another 15 minutes. After rinsing in distilled water and dried, they were viewed under the Jeol JEM-100 CX II electron microscope.

II.8. Comparison of expression of various proteins in the spinal cord

Polyacrylamide gel electrophoresis

The formulae for making the gels were obtained from Protean™ II Slab Cell (Bio-Rad, California,U.S.A.). The 10% separating gel was made up of 0.375M Tris, pH8.8, 30% acrylamide and N'N'-bis-methylene-acrylamide(bis), 10% sodium dodecyl sulfate (SDS), 10% fresh ammonium persulfate and 0.0005% N,N,N,'N'-tetramethylethylenediamine(TEMED). The mixture for the separating gel was put into a casting stand with glass plates, covered with a layer of distilled water to prevent evaporation and allowed to polymerize for 45 minutes. After the separating gel had set, excess water was pipetted out. The mixture for the 40% stacking gel (0.125M Tris, pH6.8, containing 13% acrylamide and bis, 10% SDS, 10% fresh ammonium persulfate and 0.001% TEMED) was layered above and a comb inserted at the top. The comb was removed

after the stacking gel was set.

Rats were anesthetized with 2% Nembutal (50mg/kg) intraperitoneal injection. After perfusion with 0.9% saline, a 0.5 cm long lumbar SC containing the lesion site, was dissected out. Intact spinal cord, not subjected to any lesion, was used in gel electrophoresis. The tissue was weighed and sonicated for 30 seconds in TX-100 lysis buffer (10 mM NaH_2PO_4, 110mM NaCl, 50 mM EDTA, 0.5% Triton X-100 pH 6.5), containing 1.89 g/ml aprotinin, 5mM benzamidine and iodoacetamide and 1mM phenylmethanesulfonyl fluoride. Following centrifugation at 12,000 g for 15 minutes, the supernatant was mixed with the sample buffer (62.5 mM Tris-HCl, pH 6.8, containing 10% glycerol, 2% SDS, 5% B-mercaptoethanol and 0.05% bromophenol blue) in the same volume and heated at 95^{o}C for 10 minutes.

Samples were loaded at 15 ul to each well at a concentration of 0.26 mg/ul. Prestained SDS-PAGE Standards ranging from 49,000 to 205,000 daltons (Bio-Rad, California, U.S.A.) were also applied. Electrophoresis was run at 200V for 45 minutes in the gel apparatus (model 200/2.0, power supply, Bio-Rad) with running buffer (25mM Tris, pH 8.3, containing 192 mM glycine, 0.1% SDS) diluted in 1:4 in distilled water. For staining the gel, it was immersed in fixative (Coomassie blue 1 g/l, 40% methanol, 10% glacial acetic acid) for 30 minutes. Then it was destained with destaining solution (7.5% glacial acetic acid and methanol) for 1 hour to remove the background.

Western blotting

Immunoprecipitated SC proteins were transferred from gel to nitrocellulose membrane in transblot buffer (25 mM Tris-base containing 192 mM glycine and 20% methanol) at 0.25A and 100V for 1 hour. The membrane was cut into strips corresponding to the different lanes. The strips were incubated overnight at 4°C with specific monoclonal mouse anti-GFAP antibody (Sigma). The antibody was diluted 1:400 in 0.1% Tween 20 in Tris-buffered saline (100 mM Tris, 0.9% sodium chloride, pH7.5). This buffer is called TTBS hereafter. Monoclonal mouse anti-NF antibodies (Sigma) were also applied in the same way. Neurofilament subunits of molecular weight 68,000 and 160,000 were detected with specific antibodies against them. All the dilution used was 1:100. Following overnight incubation with the various primary antibodies, the strips of membrane were rinsed with 3 changes of TTBS over 15 minutes with gentle agitation and then transferred to the solution of biotinylated secondary antibody (Vector, California, U.S.A.) (1 drop of stock in 10ml TTBS). They were incubated for 30 minutes with gentle agitation and washed as above. Then the strips were transferred to the Vectastain ABC reagent (Vector) (2 drops of avidin DH mixed with 2 drops of biotinylated horseradish peroxidase H in 10 ml of TTBS immediately and allowed to stand 30 minutes for complex formation). The strips were incubated in this solution for 30 minutes with gentle agitation and rinsed as above. After that, it was transferred to the substrate solution [25 mg

diaminobenzidine(DAB), 16.67 ul of 30% hydrogen peroxide in 50 ml TTBS]. It was allowed to react for 1 minute. When the reaction was complete, bands of brown product could be seen on the strips.

Controls were performed by incubating the strips in TTBS alone, in the absence of the primary antibodies.

Immunoblots were scanned by a Personal Densitometer (Molecular Dynamics, CA).

III. Results

III. 1. Survival of cultured astrocytes

The cultured astrocytes were shown to survive well on the gelfoam by scanning electron microscopy. Astrocytes of various shapes were present on the gelfoam. Some were spherical, while others were flat and polygonal in shape (Fig.8 and 9).

III. 2. Light microscopy

Hemotoxylin and Eosin staining

Two weeks after lesion

Two weeks after operation, traumatic necrosis marked by the presence of cystic cavities and degenerating tissue in the area around the lesion was more prominent in the HH than the HA group (Fig.10 and 11). Considerable numbers of macrophages, possessing vesiculated cytoplasm, were found in areas of necrosis, particularly in the control (HH) group (Fig.12). Reactive gliosis was already apparent and was characterized by the presence of astrocytes whose elongated nuclei stained more heavily than those of normal astrocytes. They were more numerous in the HH than the HA group (Fig.12). Lymphocytes and blood vessels were occasionally found around the lesion site in both experimental and control groups.

In the case of the HAG and HG groups, where a piece of gelfoam was placed in the lesion site, red blood cells were seen to be trapped in the gelfoam spaces. Other cell types were also apparent but they could not be definitively identified. In the region of

the gelfoam, there were always more cells and fibres in the HAG than HG group (Fig.13 and 14). Although fibres were not organized into bundles in both groups, they were more often observed to cross from the SC into the peripheral part of the gelfoam in the HAG group (Fig.13). Thus the boundary between the gelfoam and SC was not as distinct.

In the experimental (HAG) group, fewer cystic cavities and glial like cells with pale staining cytoplasm were present in the area outside the gelfoam (Fig.13).

One month after lesion

In both HH and HA groups, cystic cavities and macrophages were reduced, compared to shorter survival times (Fig.15 and 16). Lymphocytes were occasionally present in both groups. Decrease in the number of astrocytic glial cells was especially prominent in the HA group (Fig.16), while blood vessels became more numerous (Fig.16). More fibres were found in the HA group, although they resembled collagen fibres (Fig.16).

In the HAG and HG groups, fewer cells were found, compared to the 2 weeks post lesion animals. Phagocytic cells were not as easily observed as previously (Fig.17 a and b). Some surrounding tissues grew into the gelfoam and this was more prevalent in the HAG group. Among these tissues were nerve-like wavy fibres. Presence of blood vessels was more obvious in the HAG group (Fig.18a). At the same time, a mixture of fibres composing both of disorganised and organised profiles appeared in the HAG group

(Fig.18b). They resembled new nerve fibres.

Two months after lesion

At 2 months after lesion, the size and number of cystic cavities in both HA and HH groups had decreased dramatically, particularly in the HA (Fig.19 and 20). Similarly, the number of macrophages and lymphocytes was also reduced, while blood vessels were more prominent in the HA group (Fig.19). Also more organized fibres were found in the HA group extending into the lesion area.

In the HAG and HG groups, much of the gelfoam had been resorbed by 2 months after surgery (Fig.21 and 22). Fewer macrophages and glial cells were present around the lesion site than before. At this time, the control (HG) group still appeared to have slightly more cavities and gliosis around the lesion area (Fig.22) than the HAG group which had more nerve like fibres in the region (Fig.21). In the area around the original location of the gelfoam, some of these fibres were parallel to the axis of the SC. In contrast, where nerve like fibres were present in the HG group, they were more likely to be less organized and criss cross each other.

Table 1 summarizes the morphological observations on the experimental (HA and HAG) and control (HH and HG) groups from 2 weeks to 2 months after surgery.

Toluidine Blue staining

One month after lesion

Toluidine Blue staining revealed the presence of myelinated

axons which could not be observed with H & E staining. Part of the gelfoam was still present in the HAG group (Fig.23). There were more cells and nerve-like bundles in the gelfoam, compared with those of the HG group (Fig.24). On the other hand, spaces were more evident in the gelfoam of the HG group (Fig.24).

Two months after lesion

Much of the gelfoam had resorbed in both the HAG and HG groups at 2 months after surgery. There were a few cavities while much of the area shows extensive infiltration of various types of tissue. Myelinated and unmyelinated fibers were found in the region (Fig.25).

Based upon these observations, we can conclude that the morphological changes indicate a general reduction of tissue scarring over time with the emergence of nerve-like fibres in the area around the lesion after implantation of astrocytes. Tissue scarring was often more extensive in the control groups.

PHAL labelled astrocytes

Observations on the location of PHAL labelled astrocytes were made 1 and 2 weeks following injection. In the group in which PHAL labelled astrocytes were cultured on gelfoam and then implanted, the astrocytes migrated rostrally and caudally out of the gelfoam and were 4.0 mm into the SC 1 week post implantation. Usually more PHAL labelled astrocytes were present in the region of the SC caudal to the lesion (Fig.26). In subsequent week, they migrated at about the same rate further away from the site of injection.

The length of the SC traversed by the astrocytes was about 0.6 mm/day. The astrocytes normally did not migrate across to the contralateral unlesioned side. In those specimens where PHAL-labelled astrocytes were introduced as a cell suspension, by 1 week the cells had migrated more than 4.0 mm away from the injection site. Hence, the results suggest that adherence of astrocytes to gelfoam retards their migration.

Immunofluorescence staining

N-CAM

N-CAM is expressed by developing and cultured astrocytes, but its expression is normally down regulated in the mature cell (Chuong et al., 1984; Wong, 1991). Nevertheless, it has been found that at sites of nerve injury or repair, its expression can be reinduced (Martini and Schachner, 1988). The reasons for this reinduction remain unknown.

Two weeks post lesion, in the HA specimen, there were a few N-CAM positive cells around the lesion site (Fig.27). These cells were probably the cultured astrocytes that had been introduced by injection, because double labelling with GFAP showed that the N-CAM-positive cells also express GFAP (Fig.28). Many implanted astrocytes appeared to have migrated further away from the original site of injection. Surprisingly, some bright N-CAM labelled cells were also observed in the control HH group (Fig.29). Since no cultured astrocytes had been introduced in this group, the existing N-CAM expression suggests that there could possibly be some

reinduction of N-CAM expression in some cells. Similarly, there were also N-CAM positive cells in the gelfoam in the HG and HAG groups, with the density in the experimental group being considerably higher (Fig.30 and Fig.31). Although some of them have migrated out rostral and caudal to the lesion site, the results indicate that the cultured astrocytes still retained their in vitro property of expressing N-CAM up to 2 weeks of implantation.

Two months after lesion in the HA and HH groups, no N-CAM-positive cell bodies were detected around the lesion site. However, diffuse staining for N-CAM was found around the original lesion (Fig.32 and 33). Generally, immunoreactivity was more intense in the HA group in which immunoreactivity could sometimes be observed on fibrous elements. In one specimen, N-CAM staining was particularly intense in the peripheral part of the SC near the lesion where some blood vessels were located. The staining outlined the lumen of the blood vessels and the surrounding fibers (Fig.32). The N-CAM positive fibers were probably neurites.

Quite similar observations were found in the HAG and HG groups 2 months after lesion, as evidenced by the diffuse N-CAM staining around the lesion (Fig.34 and 35). Again, the staining was slightly more intense in the experimental (HAG) group. Interestingly, in one (HG) specimen in which blood vessels were found, no N-CAM staining was associated with the blood vessels.

GFAP

GFAP immunofluorescence stains for astrocytes and reveals the possible existence of astrocytic gliosis. In the control group (HH), intense staining particularly around cavities was revealed at two weeks post surgery, in addition to more diffuse staining elsewhere (Fig.36). The experimental group (HA) seemed to have less intense staining (Fig.37). In the gelfoam implanted groups (HG and HAG), a similar pattern of comparatively reduced staining for GFAP in the experimental group was also obtained (Fig.38 and 39). This was somewhat surprising in view of the fact that the HAG group had cultured astrocytes, which are GFAP-positive, in the gelfoam and also that there was more ingrowth of tissues into the gelfoam spaces after two weeks. The staining pattern suggests that much of the tissue that had grown into the gelfoam was not astrocytic gliosis.

Two months after surgery, staining intensity for GFAP around the lesion site was reduced in both HA and HH groups. It was not possible to distinguish one group from the other. The same can also be said for the HG and HAG groups in which GFAP became localized within the remnants of the gelfoam and a narrow rim of SC tissue surrounding the gelfoam (Fig.40).

NF

Two weeks after surgery, in the experimental groups of HA and HAG, NF-positive fibres could be observed in the lesion site. The fibres were irregular and appeared in a meshwork (Fig.41). More distant from the lesion site, these fibres were more regularly

arranged as fascicles and were more prominent caudal to the lesion (Fig.42). The experimental groups appeared to have more NF-positive fibres although these were also observed in the control groups (Fig.43 and 44). The presence of NF-positive fibres in the experimental groups could be observed as far as 1 month and 2 months after surgery (Fig.45) and the fibres were usually more numerous in the experimental groups.

During the course of immunofluorescence staining, the presence of autofluorescent cells was consistently observed (Fig.46) in the lesion site in all rats and at all time points. The phenomenon of autofluorescence could be a consequence of either the high number of lysosomes or lipofuchsin granules in some cells. It is not clear what functional role these cells play.

III. 3. Transmission electron microscopy (TEM)

One month after lesion

Transmission electron microscopy of blocks 2 and 3 (containing the gelfoam) in the HG and HAG groups showed that the area possessed a lot of fibroblasts in the midst of collagen fibres (Fig.47 and 48). The fibroblasts were characterised by expanded rough endoplasmic reticulum. At this stage, many phagocytes were observed in the HG group. They were in the process of engulfing gelfoam and the perikaryon contained lysosomes (Fig.49). Phagocytes were comparatively less frequently observed in the HAG group and they were usually found in close association with the gelfoam matrix (Fig.50). There were few bundles of neurites in the

control and experimental groups. Occasionally, neurites with lots of neurofilaments inside were ensheathed by glial-like cells (Fig.51). In addition to neurites, clusters of myelinated axons interspersed with unmyelinated axons could be observed in the HAG group (Fig.52). Interestingly, when blood vessels were observed, they were often in the vicinity of myelinated axons (Fig.53). Well defined synapses were not observed although in some instances electron dense regions were present between two apposing processes containing vesicles, perhaps suggesting the early formation of synapses (Fig.54).

Two months after lesion

In blocks 2 and 3 of the experimental HAG group, a large number of both myelinated and unmyelinated nerve fibres was found. Some of the unmyelinated fibres were axons as evidenced by the presence of microtubules while others appeared to be less differentiated neurites as indicated by the presence of large numbers of neurofilament (Fig.55). Synapses between axon terminals and dendrites were also found (Fig.56).

In the control (HG) group, 2 months after lesion, myelinated nerve fibres were also present. However, many of them appeared abnormal because the axon ensheathed within were either degenerating or shrunken (Fig.57). Consequently large spaces were found within the myelin sheath which was often distorted into odd shapes. Also, layers of the myelin sheath were disrupted at certain sites. Synapses were less frequently observed in the

control (HG) group.

In block 4 (caudal to lesion), normal looking bundles of neurites with synapses were more easily seen in the experimental (HAG) than control (HG) group (Fig.58 and 59). On the other hand, myelinated axons were less frequently observed in the experimental group (Fig.58). Some of the myelinated axons in the control group appeared to be degenerating (Fig.59), and very few synapses were observed.

Compared to block 4 ultrastructural observation of block 1 of experimental and control groups showed a lower density of neurites and both myelinated and unmyelinated axons. Synapses were not observed.

III.4. Determination of the volume of scar tissue

The volume of scar tissue in the various groups at different time post surgery is shown in Fig.60. The volume of scar tissue at the lesion site decreased from 2 weeks to 2 months after surgery in all groups. The rate of reduction for experimental and control groups is similar. That is, 20-fold decrease in the HA and HH groups, and 14-fold decrease in the HAG and HG groups. But at the very beginning 2 weeks post operation, the volume of scar tissue in HA and HAG groups was already significantly reduced, compared with their respective controls. So at all time points after surgery, the volume of scar tissue at the lesion site was decreased in the experimental groups and was consistently less than that in the

control groups. Therefore, the evidence indicates that the implanted astrocytes had little to do with the rate of reduction in scar tissue from 2 weeks to 2 months post operation. But somehow they did exert the effect in limiting tissue scarring within the first two weeks following injury.

III.5. Gel electrophoresis

Various molecular weight (MW) bands of proteins in the experimental and control groups at 2 months after operation were detected. Distribution of the protein bands from the HA and HH groups were similar to that from the normal SC (Fig.61 and 62). Most prominently were two protein bands corresponding to molecular weights 180,000 (a in Fig.62) and 130,000 (b in Fig.62), followed by a series of protein bands ranging from 80,000 to 35,000 daltons (c to d in Fig.62).

III.6. Immunoblotting and densitometry

Since the gel electrophoresis only shows the distribution of proteins according to molecular weight (MW), two proteins having the same MW could precipitate in one band. In order to obtain further resolution of proteins, Western blotting was used. Densitometry tracings showed that there was a comparatively lower quantity of GFAP in the HA (Fig.63), i.e. 37% of control value (Fig.64 and 65). Since GFAP is expressed by astrocytes, the lower value in the HA group suggests that there is less reactive astrogliosis.

Antibody against NF 68 and 160 kd was applied to the HA and HH

groups. Experimental evidence in CNS and PNS neurons shows that the smaller subunit usually appears before the larger subunit during development (Carden et al., 1987; Figlewicz et al., 1988). Darker and broader bands of both NF 68 and 160 kd were found in the HA group, compared with that in the HH group (Fig.66). Densitometry tracings of these bands confirmed that the experimental group had more NF 68 (155% of control) (Fig.67 and 68) and NF 160 (124% of control) (Fig.69 and 70). This indicated that there were more nerve fibres in the lesioned HA group than the control group.

Fig1

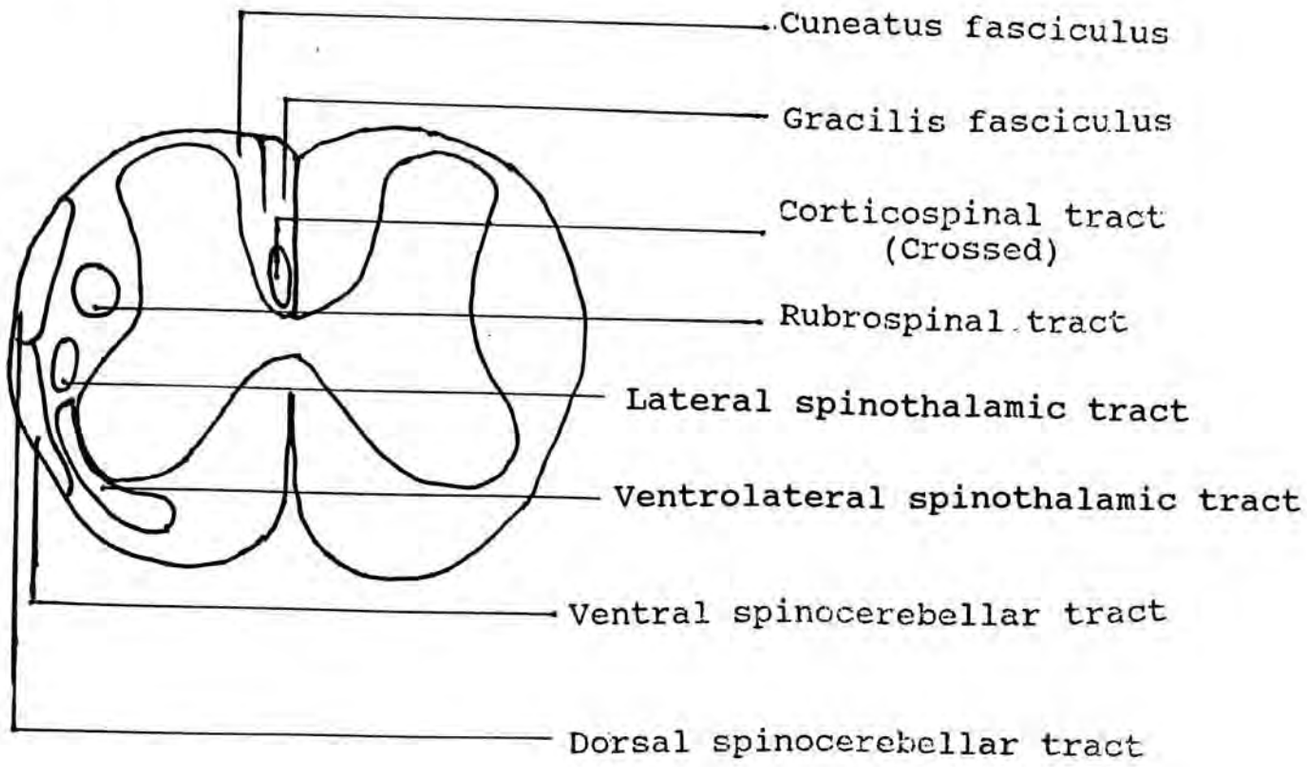

Schematic drawing of the Sensory and Motor pathways at L_3 spinal cord.

[Diagram redrawn from Vahlsing and Feringa (1980); Grant 1985; Tracey 1985; Zhang 1986]

Fig.2. Hemisection with cultured astrocyte suspension injected (arrowhead) at the time of lesion (HA).

Fig.3. Hemisection with immediate implantation of gelfoam (arrowhead) containing astrocytes (HAG).

The median dorsal artery serves as a landmark for the medial edge of the lesion.

Fig 2 and 3

Fig.4. HA, 2 months post lesion. The dotted line demarcates the boundary of the scar tissue. Bar = 24 um.

Fig.5. HG, 2 months post lesion. The dotted line demarcates the boundary of the sacr tissue. Bar = 12 um.

Fig4and 5

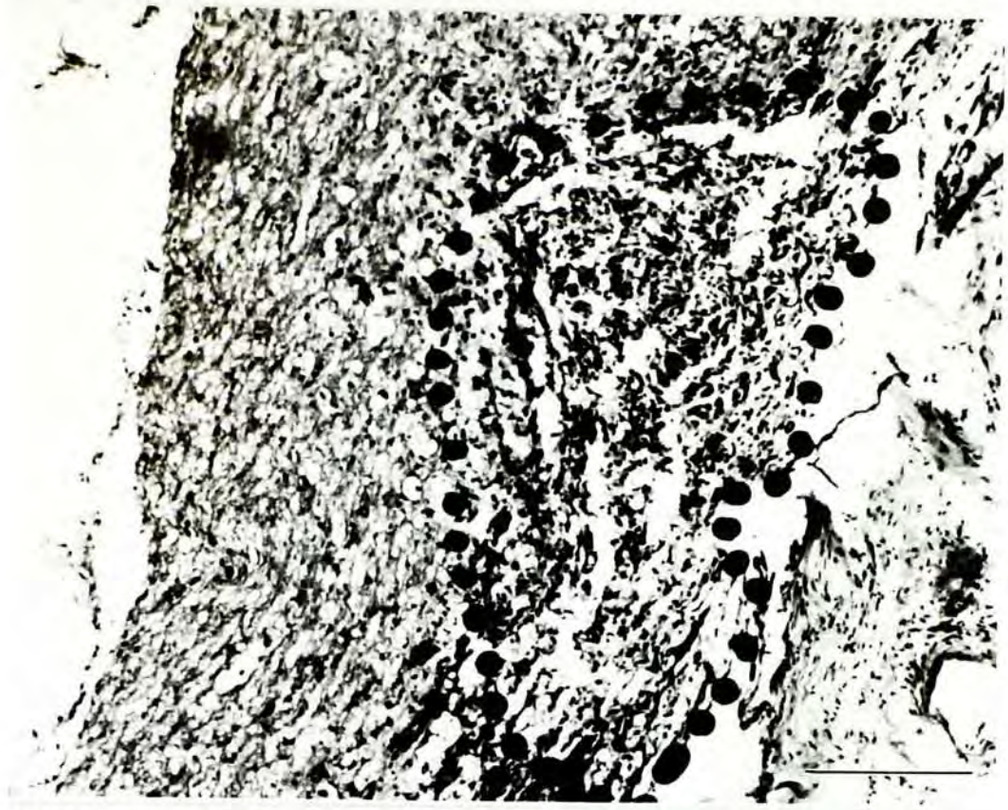

Fig.6. Astrocytes labelled with plant lectin Phaseolus vulgaris leucoagglutinin (PHAL) conjugated with FITC. Bar = 29 um.

Fig 6

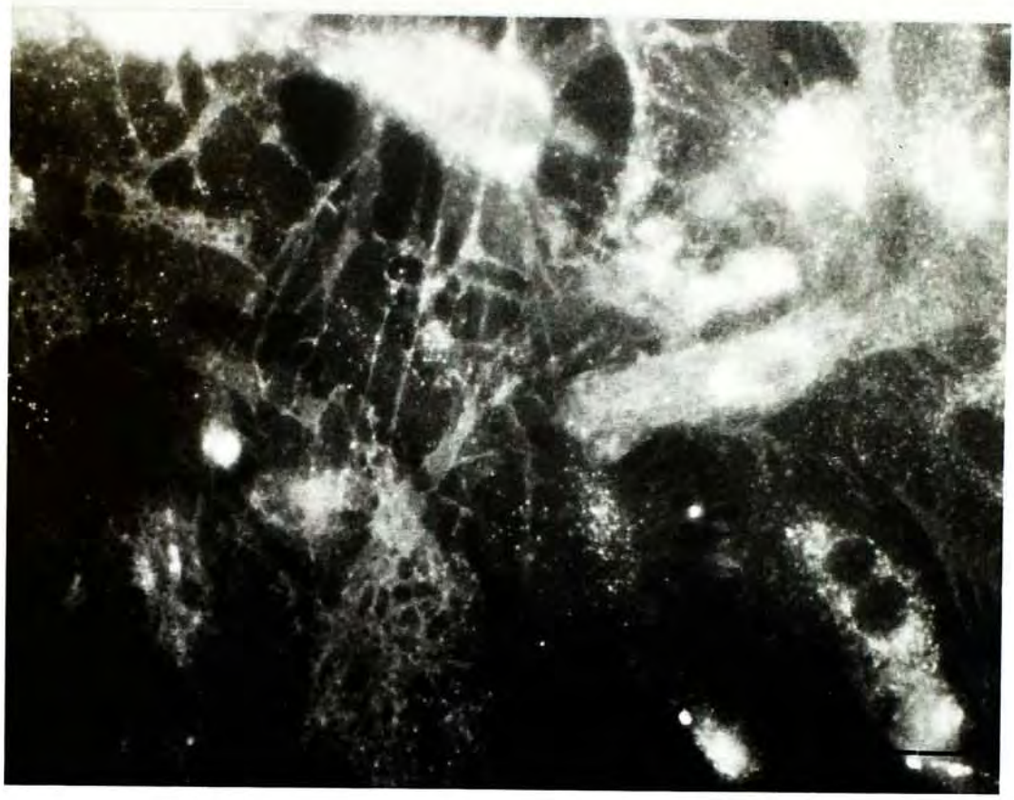

Fig7

Schematic drawing showing the designation of various blocks of spinal cord in relation to the lesion

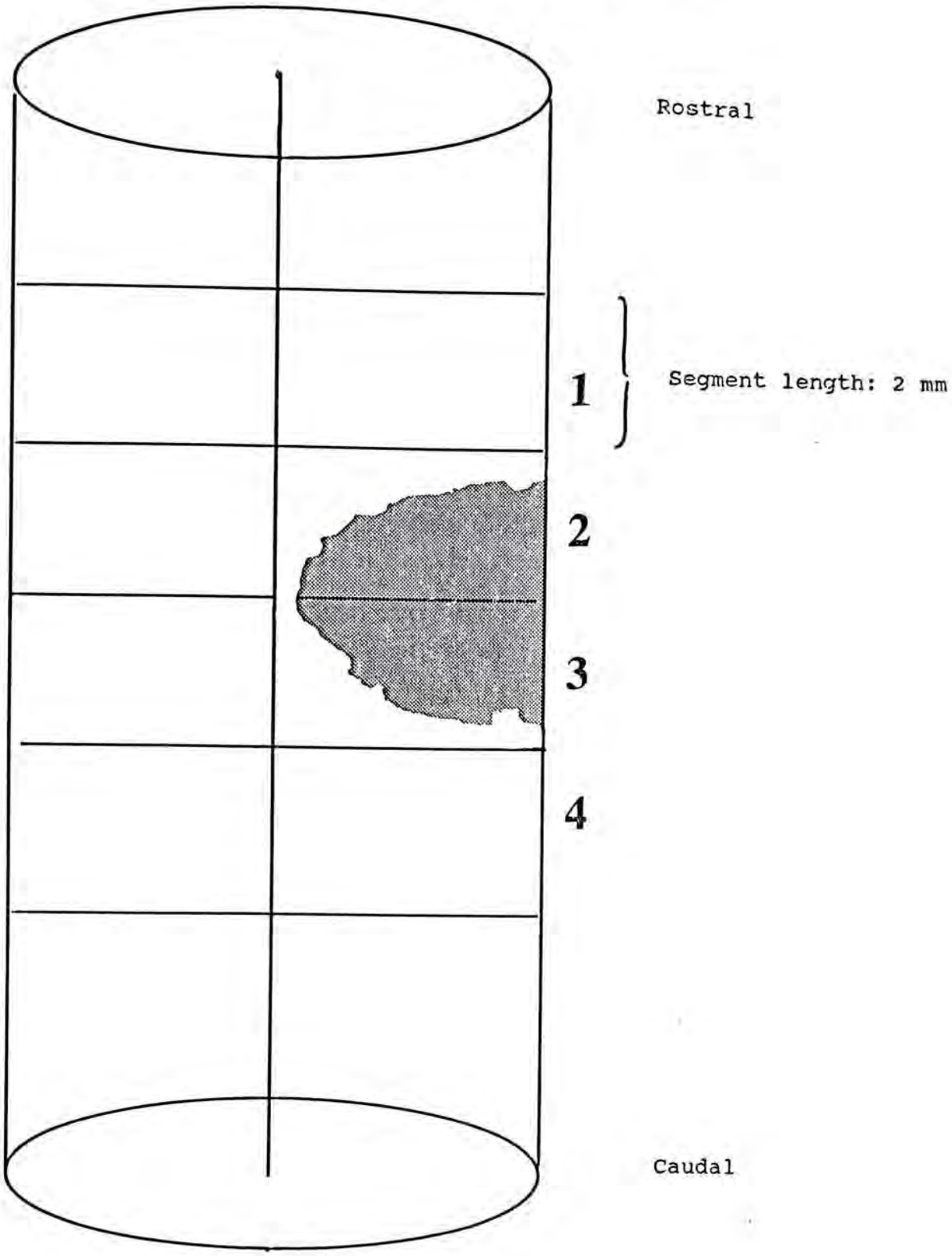

Shaded area indicates original location of gelfoam

Fig.8 and 9. Scanning electron microscopy showing the presence of cultured astrocytes on gelfoam 4 days after plating. Astrocytes of various shapes are present on the gelfoam. Some are spherical (arrowheads), while others are flat (arrows) in shape. Bar = 5 um (Fig.8); Bar = 6um (Fig.9)

Fig 8 and 9

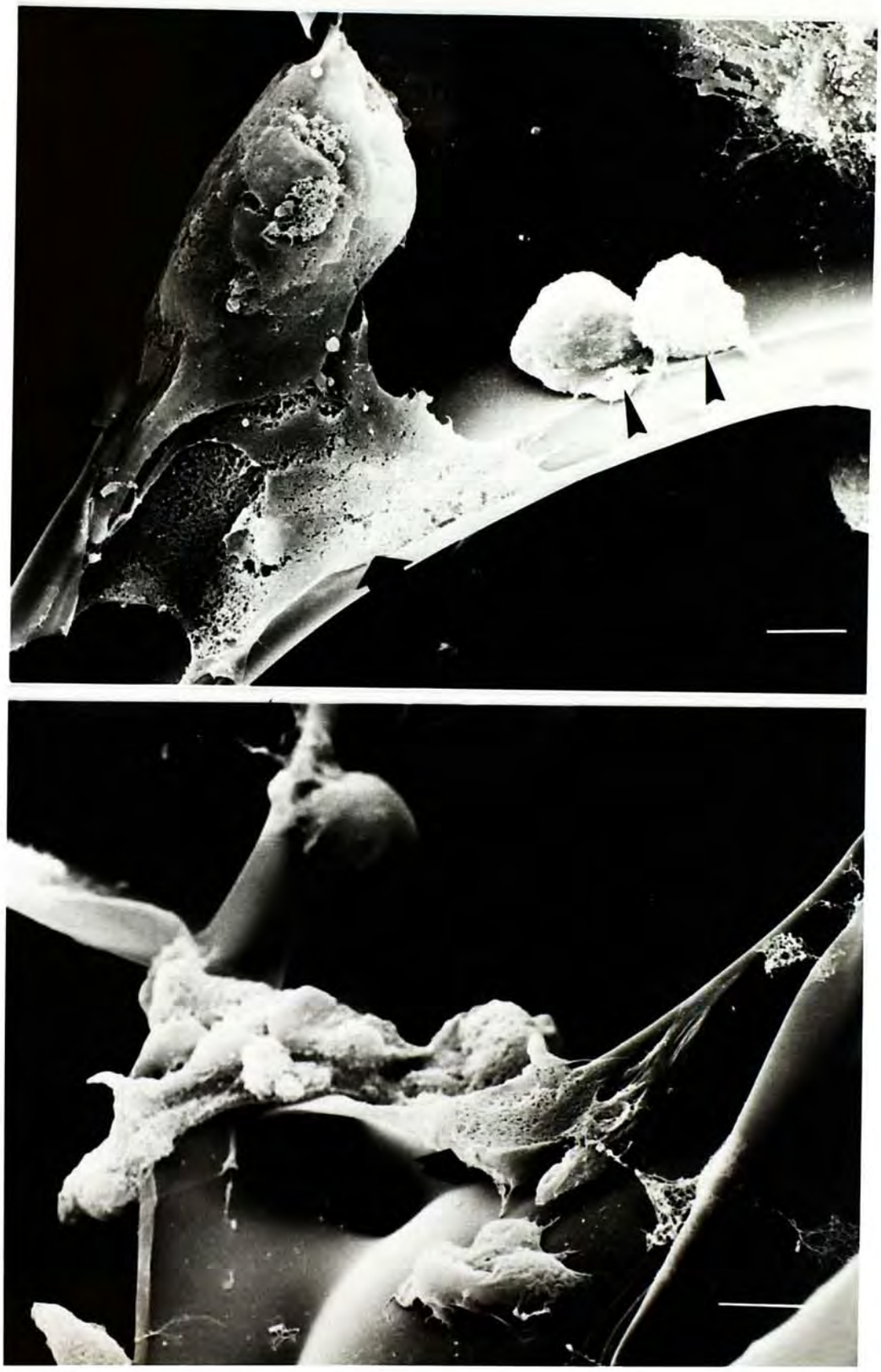

Fig.10 (Upper left) and Fig. 11 (Upper right).

HH, 2 weeks post lesion. Traumatic necrosis is marked by the presence of cystic cavities (C) and degenerating tissue in the area around the lesion. Large numbers of macrophages (arrowhead), possessing vesiculated cytoplasm, are found in the area of necrosis. Reactive astrogliosis is already apparent. Bar = 32 um.

Fig.12 HA, 2 weeks after lesion. There are fewer macrophages and less reactive gliosis. Bar = 29 um.

Fig10, 11 and 12

Fig.13. HAG, 2 weeks after lesion. Compared to the control (HG) lesion site contains, more cells and disorganized fibres (F), fewer cystic cavities and glial like cells with pale staining cytoplasm. G represents gelfoam. Bar = 29 um.

Fig.14. HG, 2 weeks after lesion. Fewer cells and fibres (F), and more cystic cavities and astroglial cells are observed in the control group. Arrowhead indicates gelfoam. Bar = 29 um.

Fig 13 and 14

Fig.15.HH, 1 month after lesion. Cystic cavities and macrophages are reduced. Arrow indicates fibroblast. Bar = 29 um.

Fig.16.HA, 1 month after lesion.

(a) There is decrease in the number of astrocytic glial cells while blood vessels (b) become more numerous. Bar = 10 um.

(b) Fibres (F) resembling collagen fibres are found. Bar = 29 um.

Fig15,16 a andb

Fig.17aHAG, 1 month after lesion. The number of phagocytic cells (arrowhead) decreases with time. Bar = 29 um.

Fig.17bHG, 1 month after lesion. The number of macrophages (arrowhead) decreases with time. Bar = 29 um.

Fig17a and b

Fig.18aHAG, 1 month post lesion. Nerve like wavy fibres are present. Presence of blood vessels (b) is more obvious than in the control group. Bar = 29 um.

Fig.18bHAG, 1 month post lesion. A mixture of fibres (arrow) composing both of disorganized and organized profiles are apparent in this area. They resemble new nerve fibres. Bar = 29 um.

Fig1 & a and b

Fig.19 HA, 2 months after lesion. Bar = 29 um.

Fig.20 HH, 2 months after lesion.

The size and number of cystic cavities in both groups have decreased dramatically, particularly in the experimental group. Blood vessels (b) are more prominent in the HA group too. In addition, more organized fibres are found in the experimental group extending into the lesion site. Bar = 29 um.

Fig19 and 20

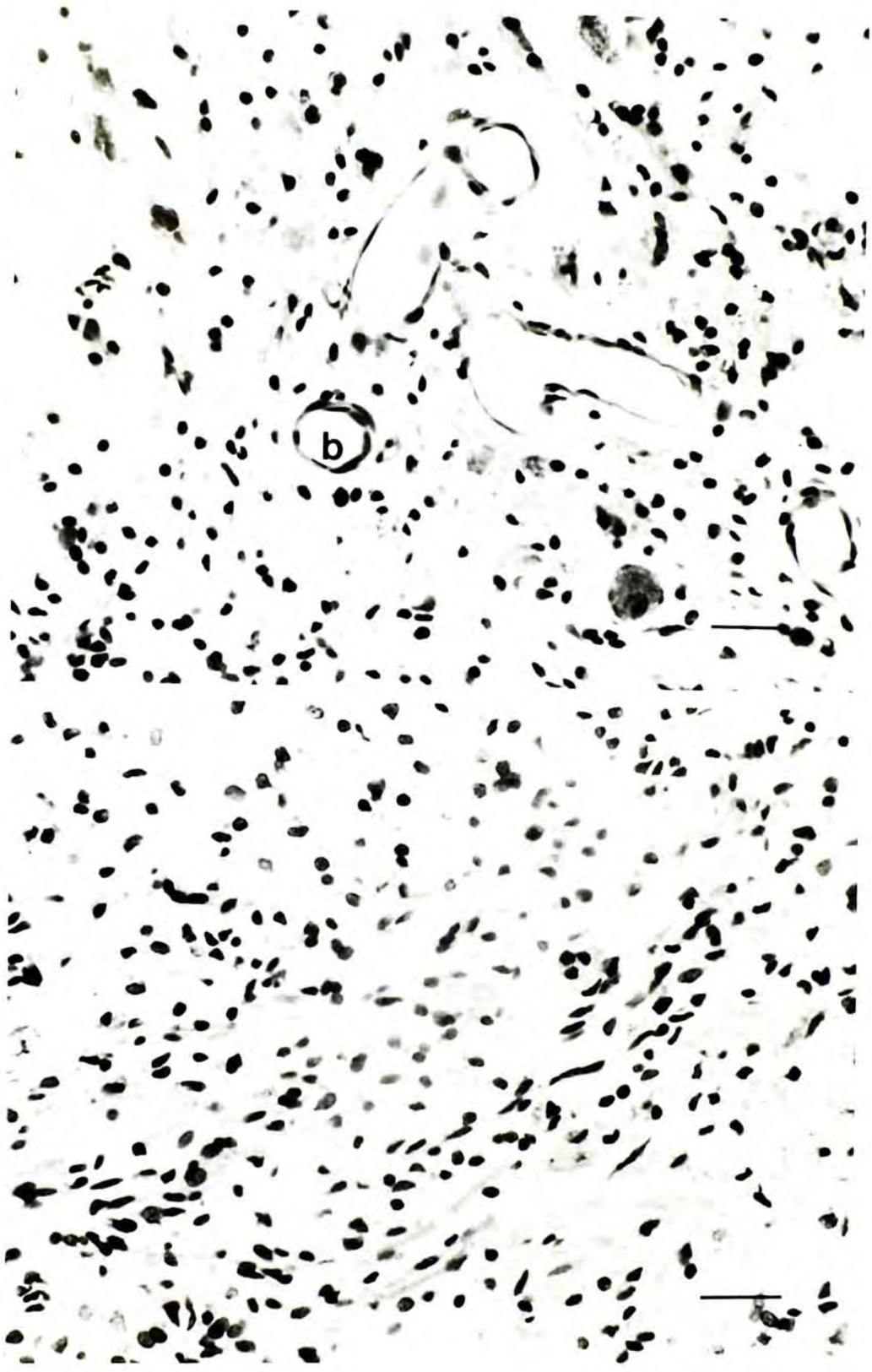

Fig.21 HAG, 2 months post lesion. Bar = 29 um.

Fig.22 HG, 2 months post lesion.

Much of the gelfoam is resorbed in both groups. HAG has more nerve like fibres (F) parallel to the axis of the spinal cord in the region of injury while HG still appears to have slightly more cavities and gliosis (arrow). The nerve fibres in HG are less organized and criss cross each other. Bar = 29 um.

Fig21 and22

Fig.23(left)HAG, 1 month post lesion.

Fig.24(right)HG, 1 month post lesion.

Toluidine blue staining. Myelinated fibres (arrowheads) are present in both groups. Fibres are prominent in the HAG group while spaces can be found in the HG group. Bar = 25 um.

Fig.25 (Lower)HAG, 2 months after lesion, Toluidine blue staining. Much of gelfoam is resorbed and there are few cavities left. Various types of tissue are observed. Myelinated fibres (n) are present. Bar = 12 um.

Fig23, 24 and 25

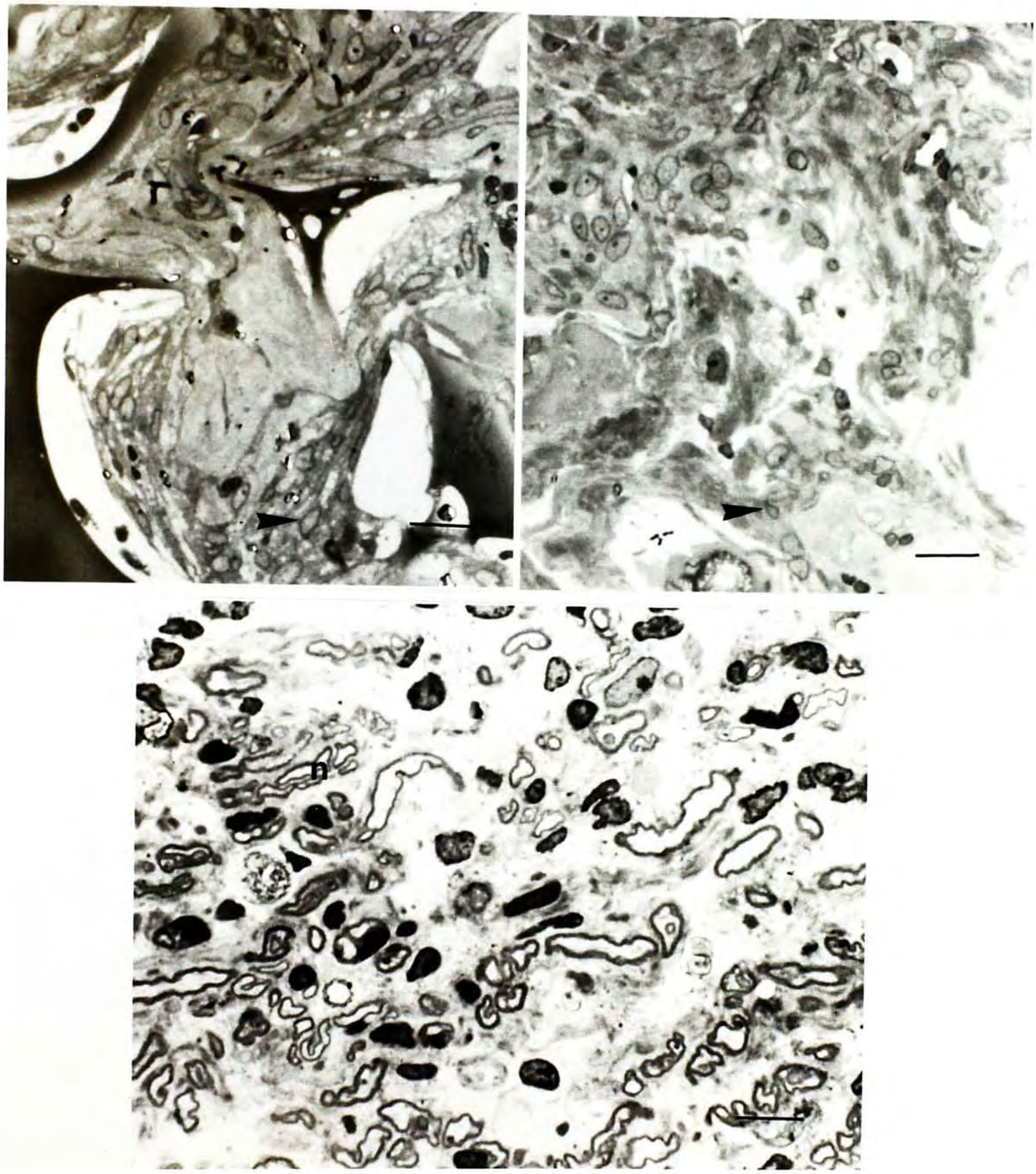

Fig.26 Astrocytes (A) labelled with PHAL are found in region caudal to lesion at one week after implantation. Bar = 29 um.

Fig26

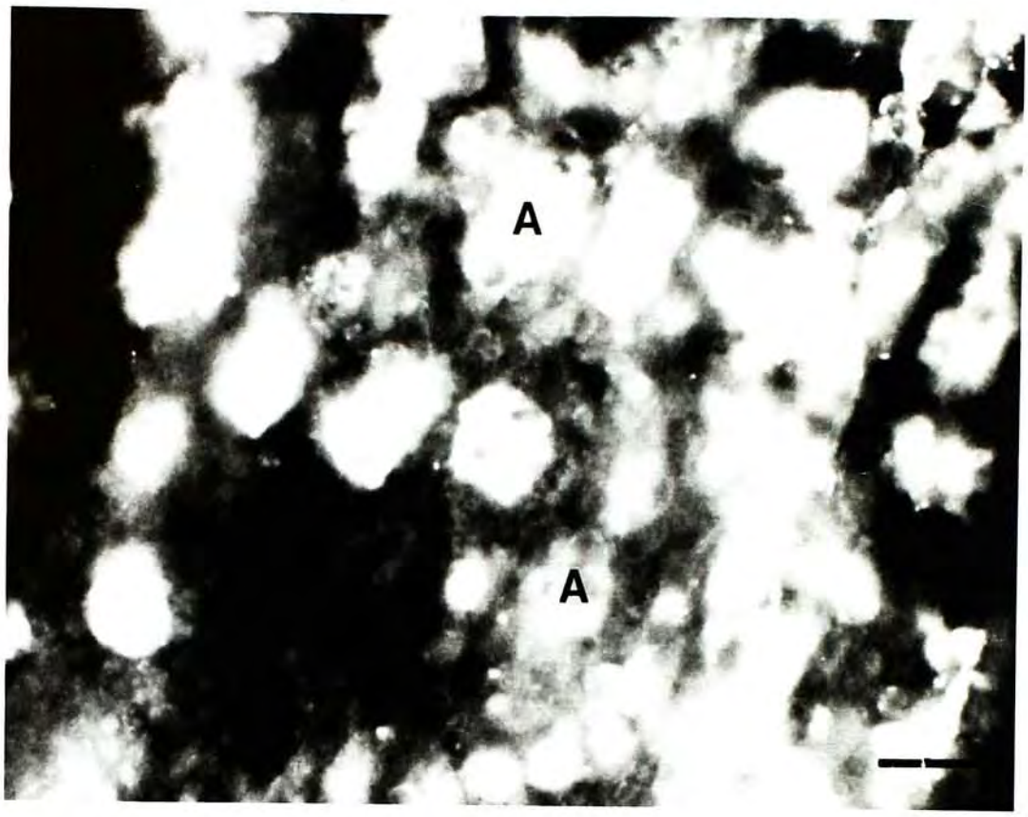

Fig.27 HA, 2 weeks after lesion. N-CAM staining. There are a few N-CAM positive cells (arrowhead) around the lesion site. Bar = 29 um.

Fig.28 HA, 2 weeks after lesion. Double labelling with anti-GFAP and anti-N-CAM. The N-CAM positive cells are also shown to express GFAP (arrowhead). However, not all GFAP positive tissues are stained for N-CAM. Bar = 29 um.

Fig27 and 28

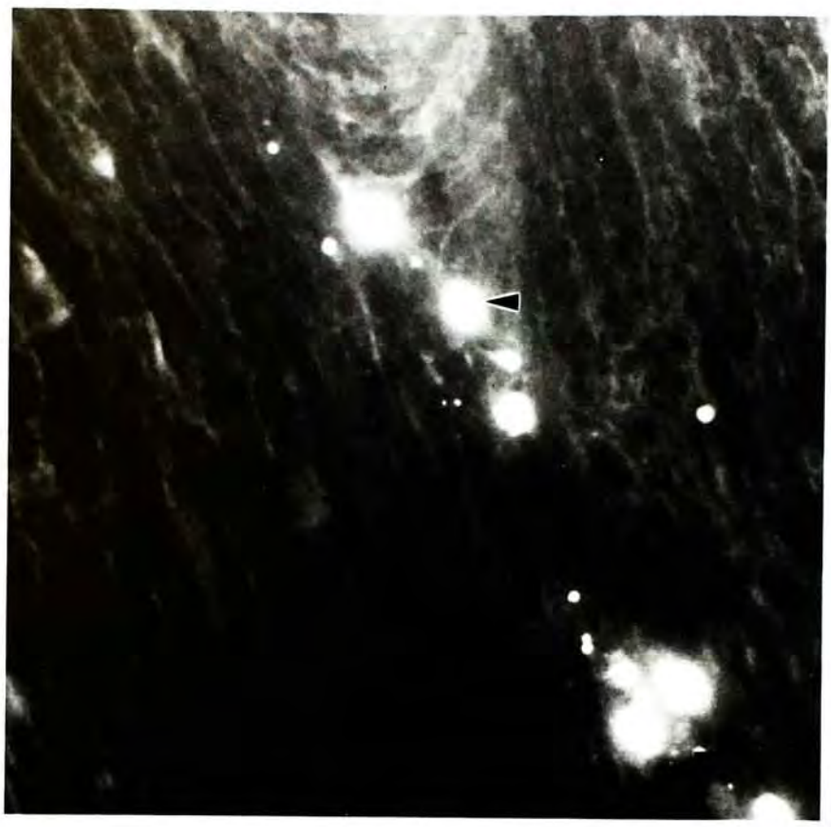

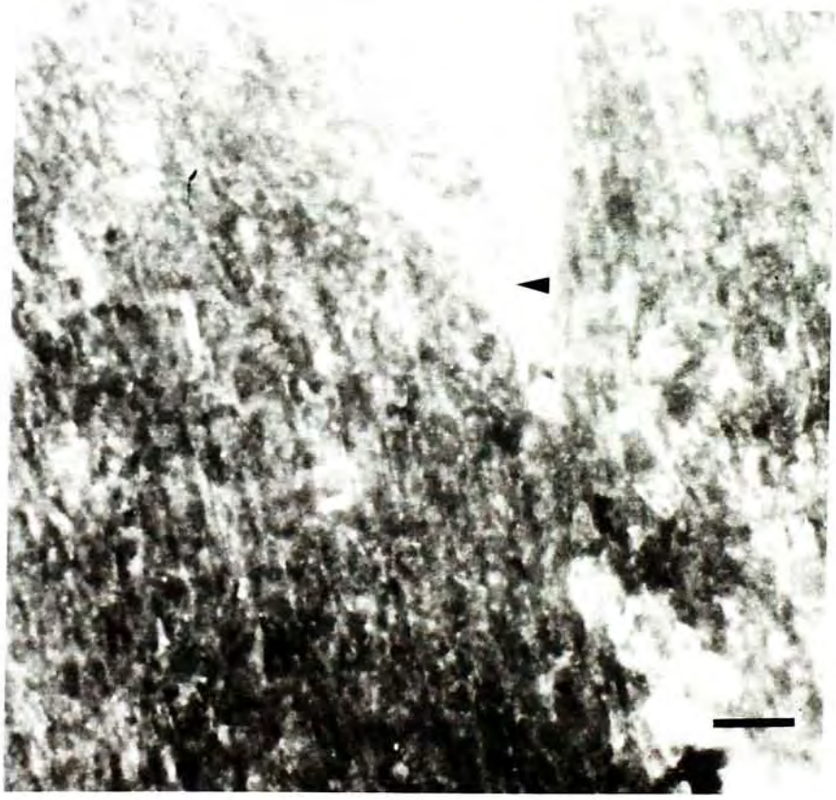

Fig.29 HH, 2 weeks after lesion. N-CAM staining. Some bright N-CAM labelled cells (arrowheads) are observed. These may be cells which have been reinduced to express N-CAM. Bar = 29 um.

Fig29

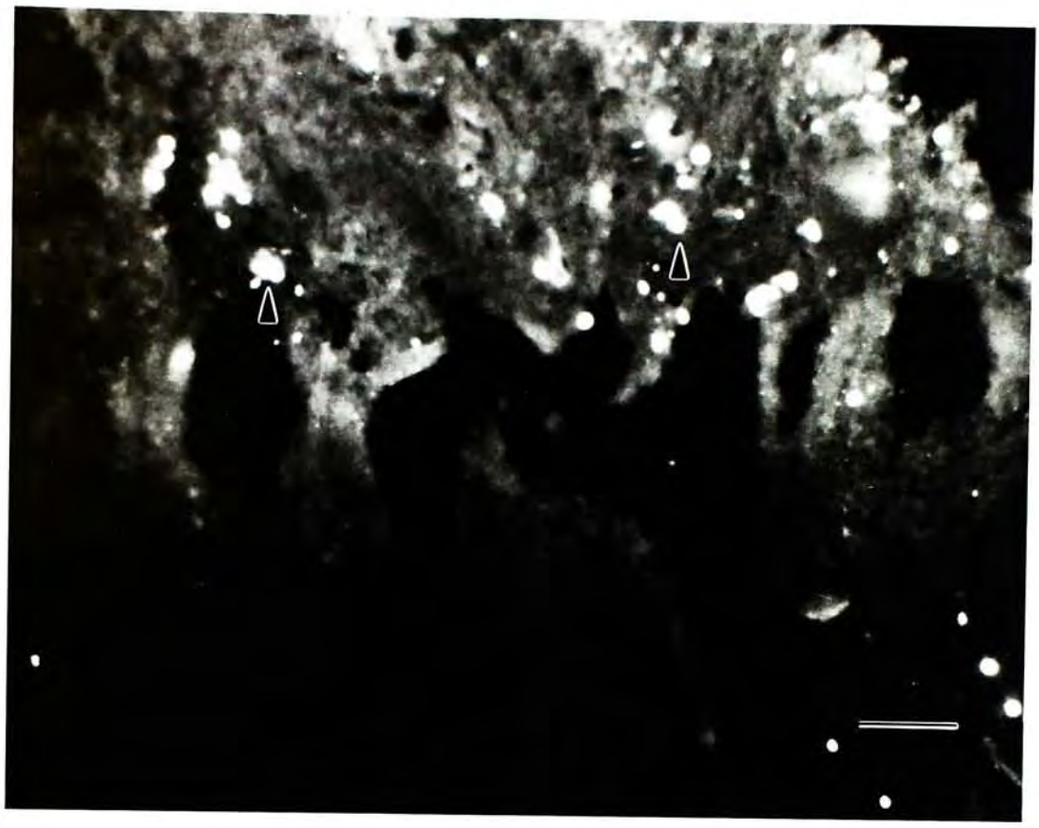

Fig.30 HG, 2 weeks after lesion. N-CAM staining. There are N-CAM positive cells (arrowhead). Bar = 118 um.

Fig.31 HAG, 2 weeks after lesion. The density of N-CAM positive cells (arrowheads) is higher than that of the HG group. Bar = 118 um.

Fig30 and 31

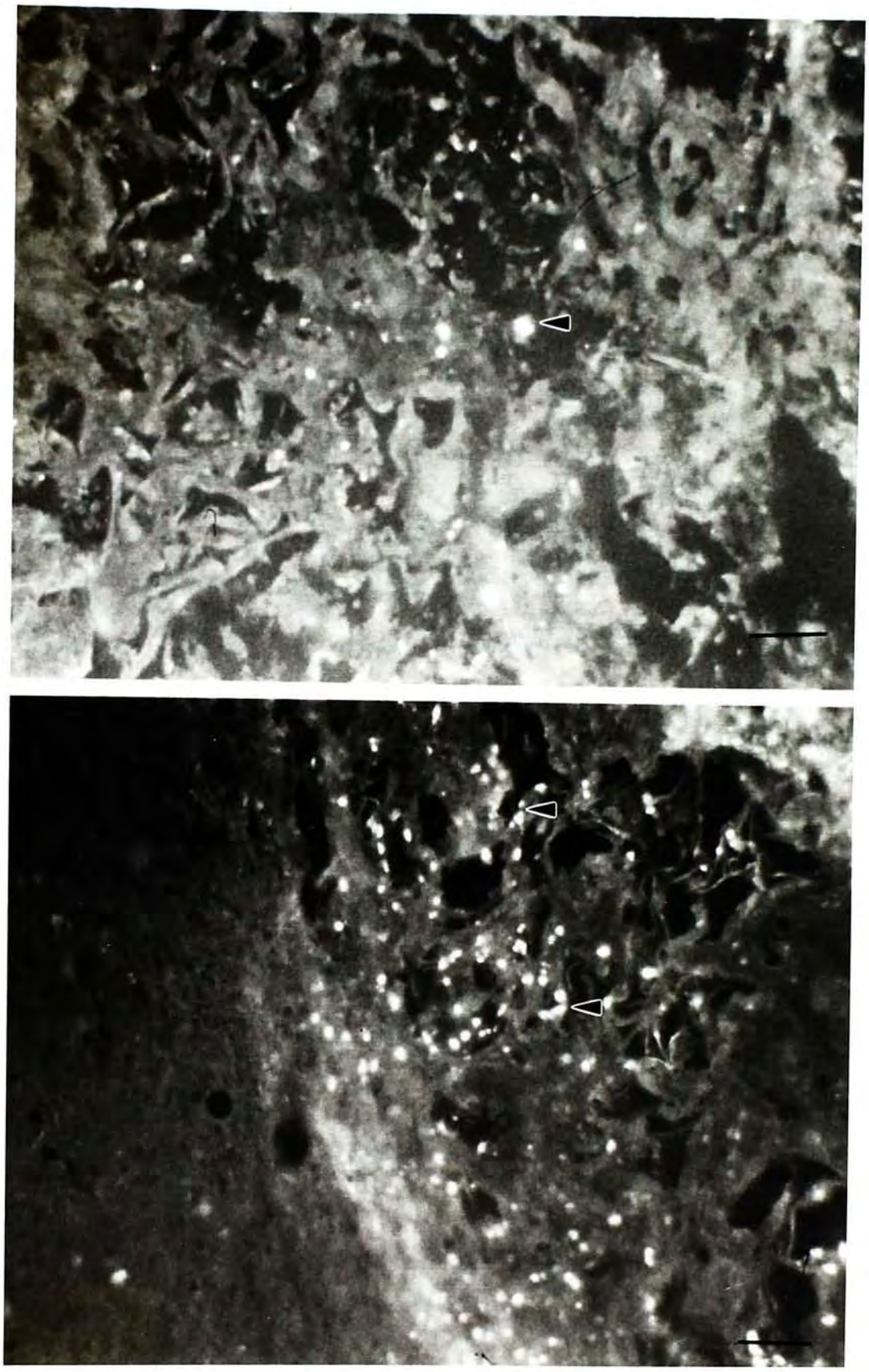

Fig.32 (HA) and Fig.33 (HH), 2 months after lesion.

Diffuse N-CAM staining is detected around the original lesion site in the HA and HH groups, with comparatively more intense reaction in the experimental group, particularly around blood vessels (arrowheads). Bar = 40 um (Fig.32); Bar = 80 um (Fig.33).

Fig 32 and 33

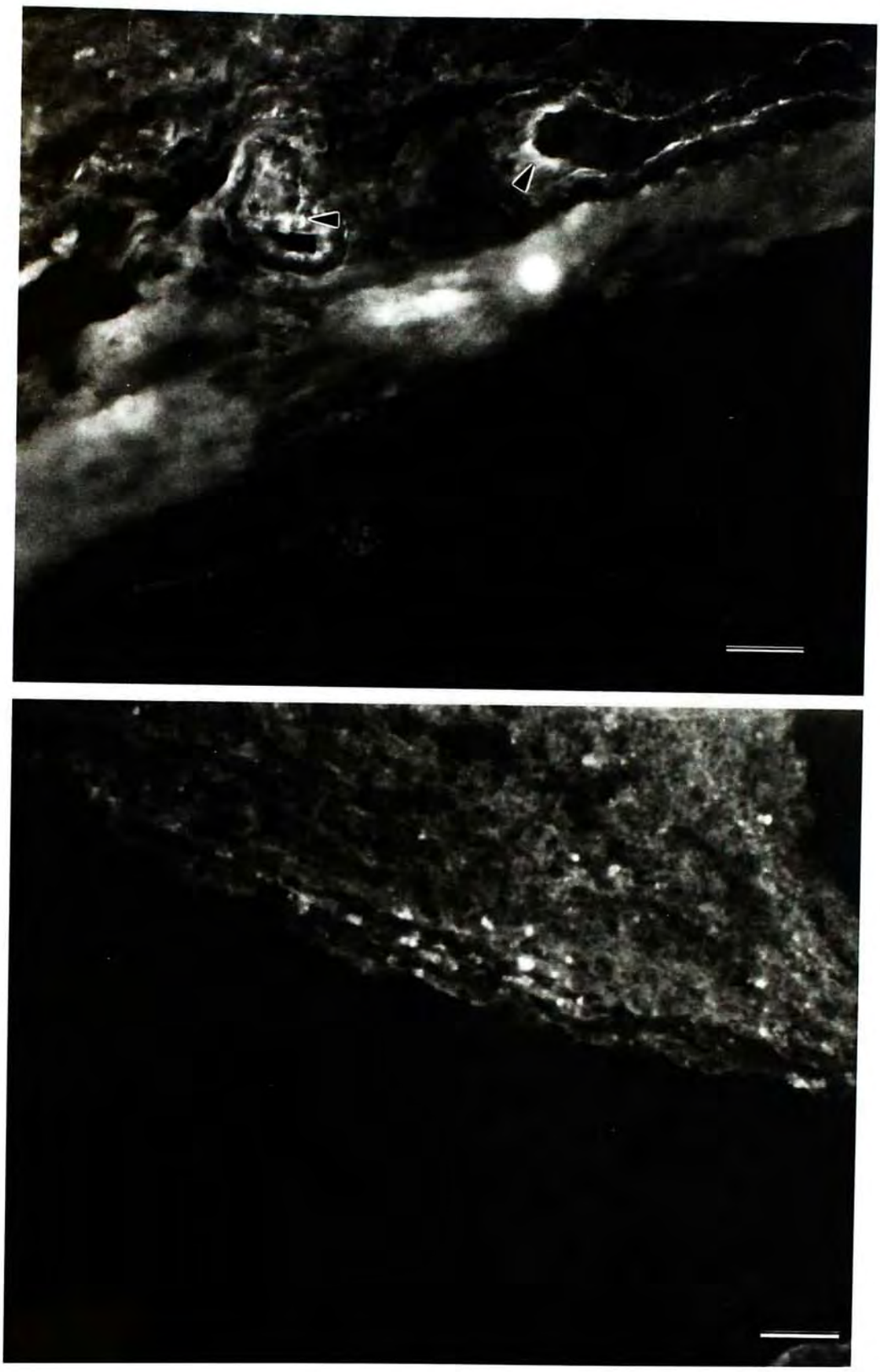

Fig.34 (HAG) and Fig.35 (HG), 2 months after lesion. Figures show diffuse N-CAM staining (arrowheads) around the lesion area. The staining is slightly more intense in the experimental group. Bar = 67.8 um (Fig.34); Bar = 40 um (Fig.35).

Fig34 and35

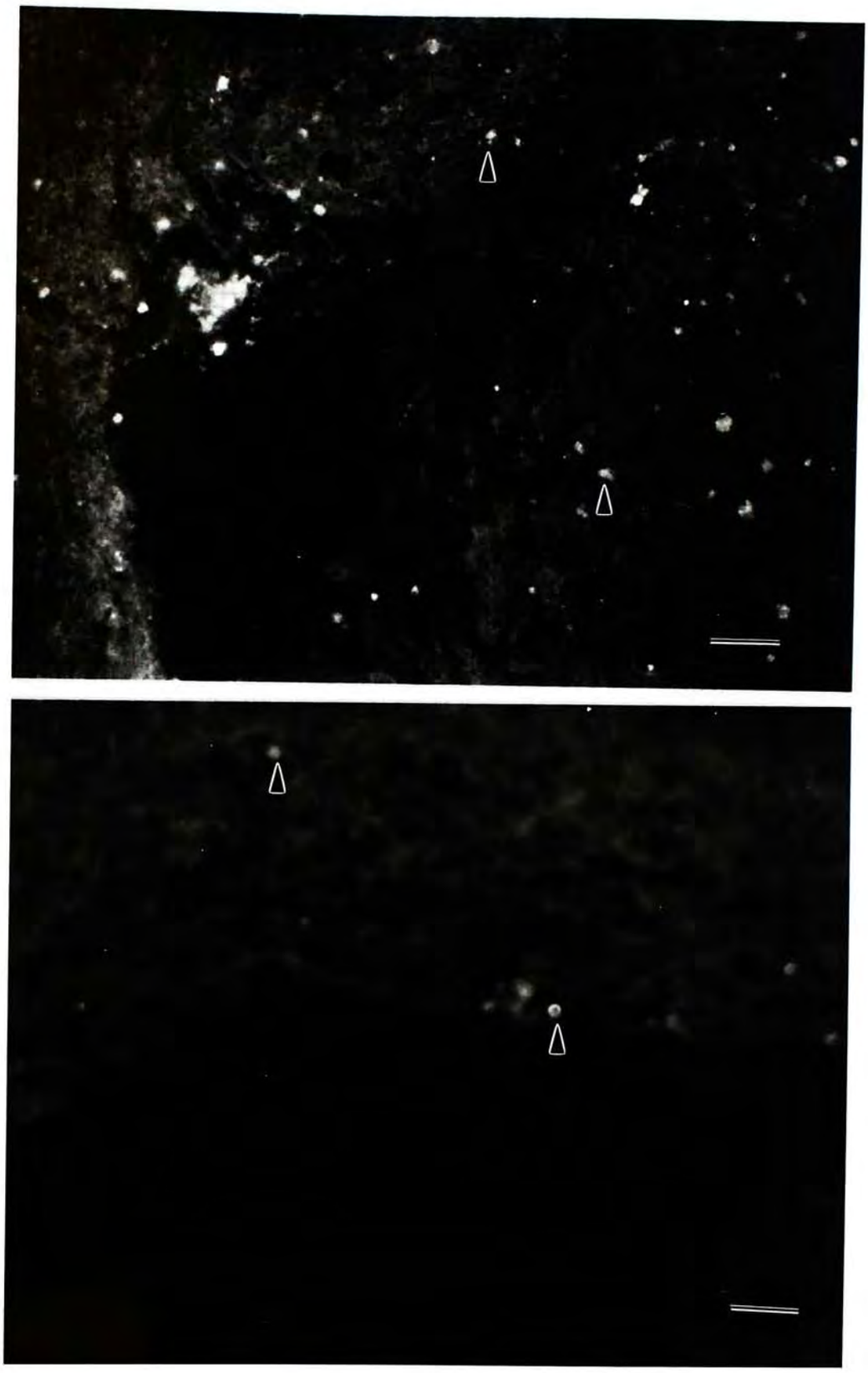

Fig.36 (HH) and Fig. 37 (HA), 2 weeks after lesion. GFAP staining. Intense staining for GFAP (arrowheads) is located around the lesion site. Staining was most prominent around the cavities in the control group. Bar = 29 um.

Fig 36 and 37

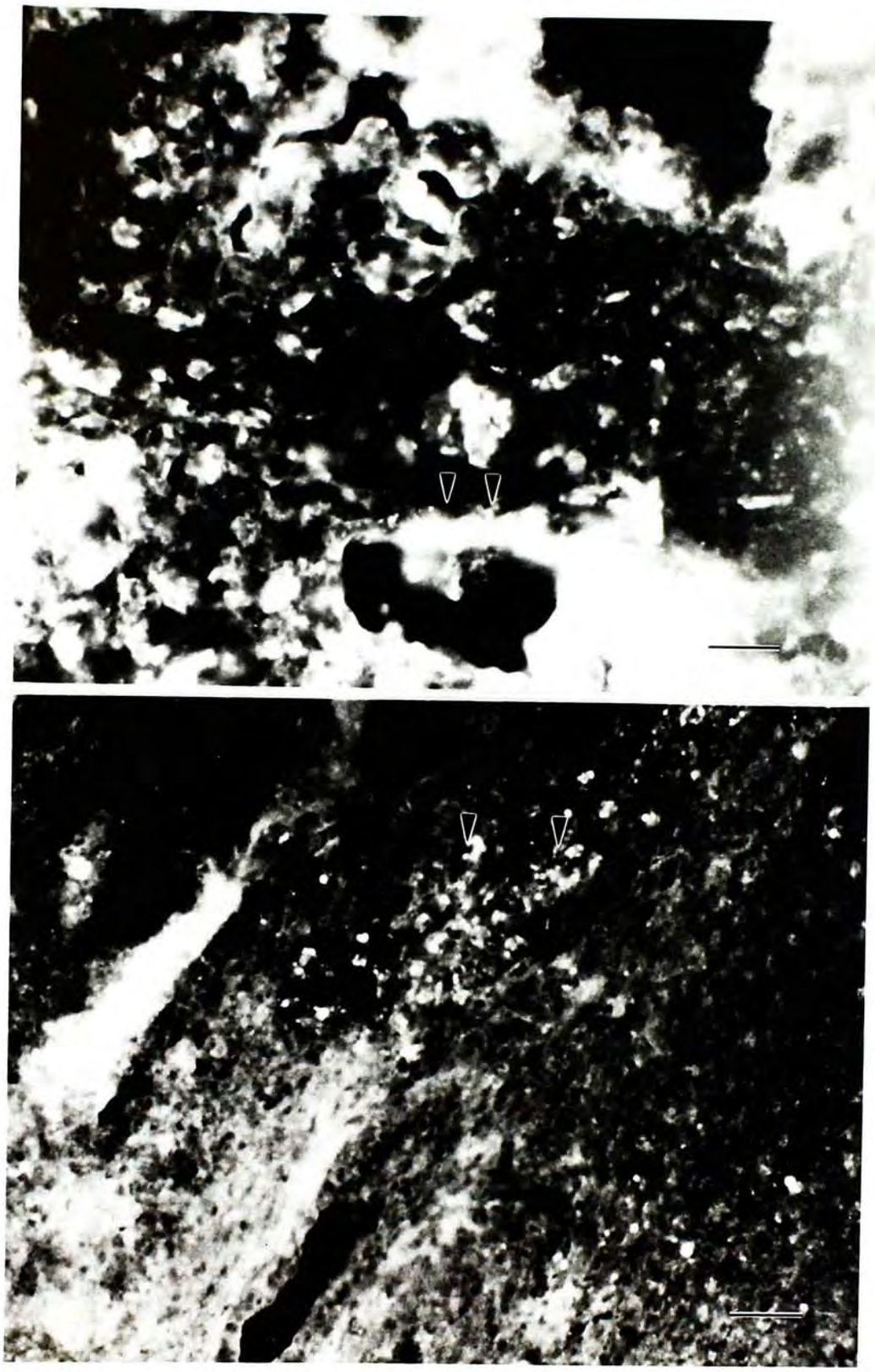

Fig.38 (HG) and Fig. 39 (HAG), 2 weeks after lesion.

Compared with the control group (Fig.38), reduced staining for GFAP (arrowheads) is observed in the experimental HAG group. Bar = 29 um.

Fig 38 and 39

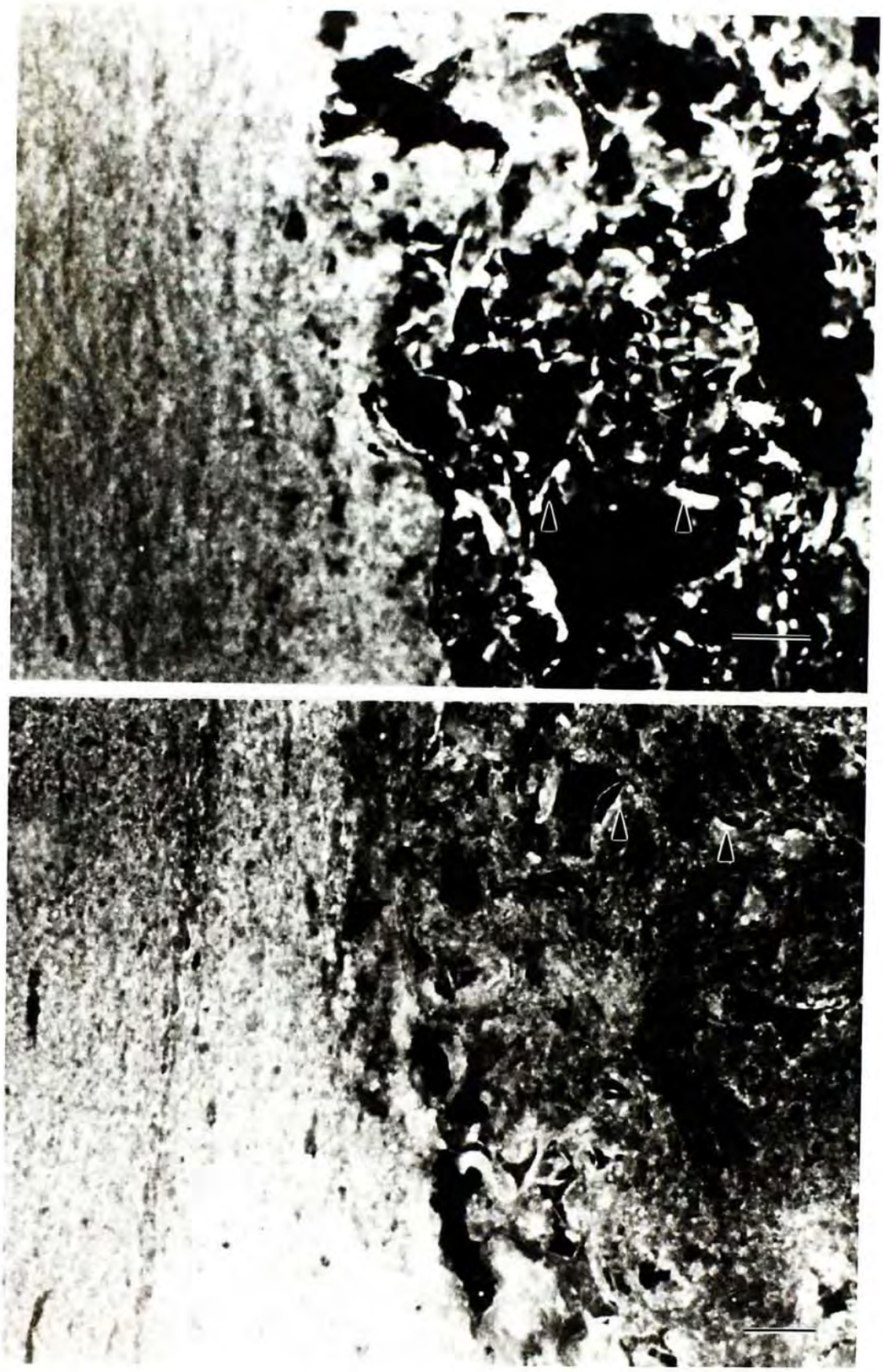

Fig.40 HG, 2 months after lesion. Labelling intensity for GFAP (arrowheads) around the lesion area is decreased. Bar = 118 um.

Fig40

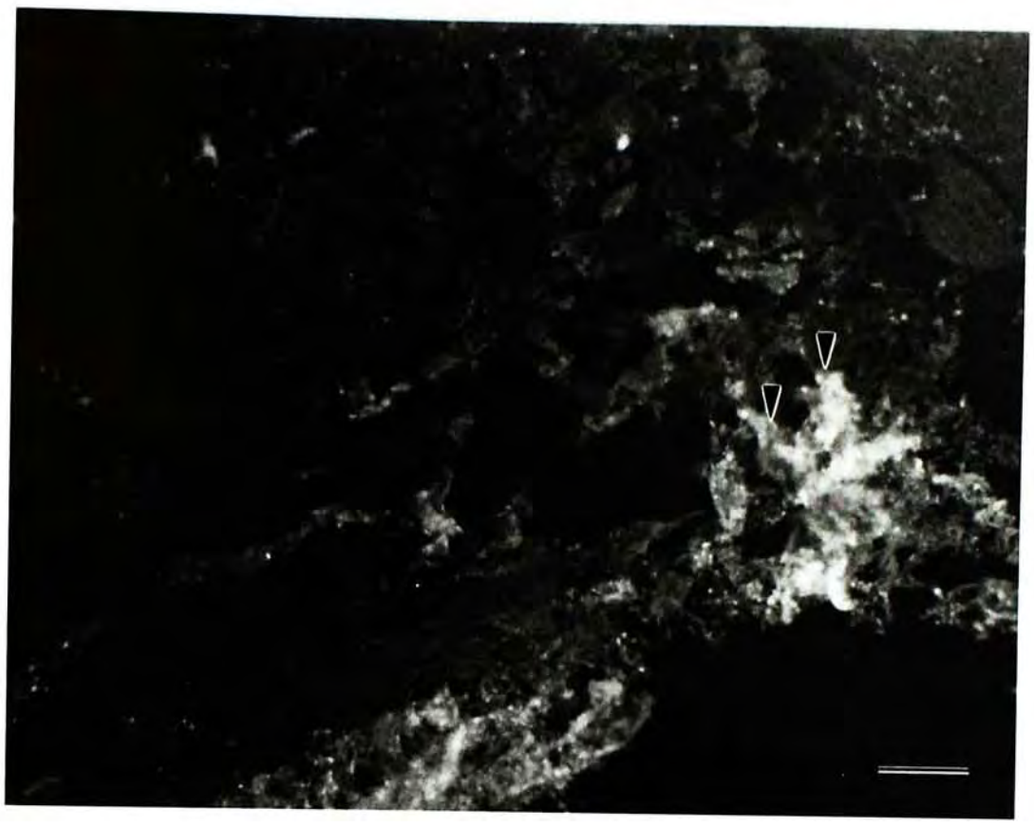

Fig.41 HA, 2 weeks after lesion. NF positive fibres (arrowheads) in the lesion site. The fibres are irregular and appear in a meshwork. Bar = 29 um.

Fig.42 HA, 2 weeks after lesion. NF positive fibres (arrowheads) are more prominent in region caudal to lesion. Bar = 29 um.

Fig41 and42

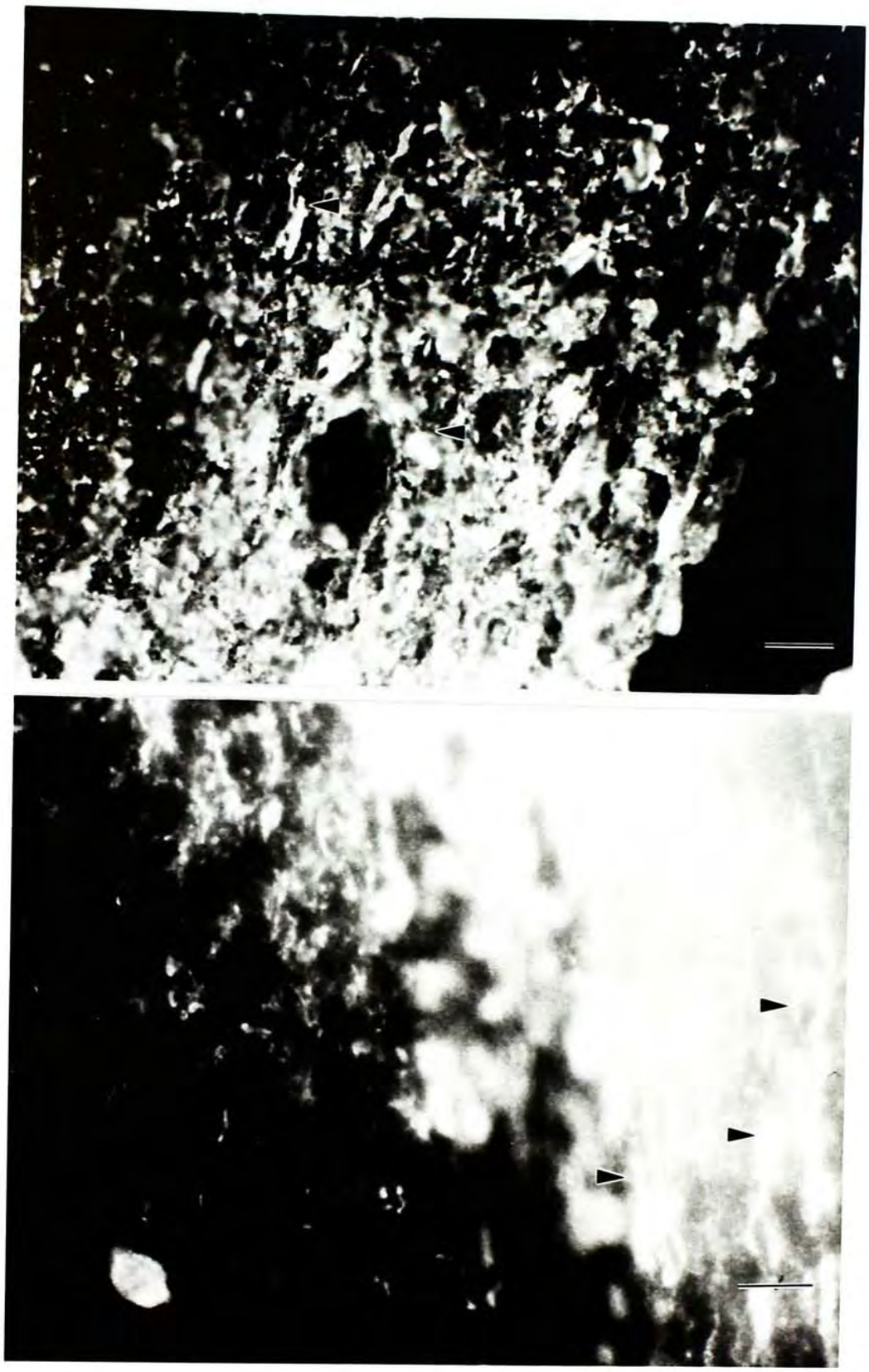

Fig.43 HG, 2 weeks after lesion. HG group has fewer NF positive fibres (arrowheads) in the lesion site than the experimental group. Bar = 29 um.

Fig.44 HG, 2 weeks after lesion. NF positive fibres (arrowheads) are evident in region caudal to lesion. Bar = 29 um.

Fig43and44

Fig.45 HAG, 2 months after lesion. NF positive fibres (arrowheads) are usually more numerous in the experimental group. Bar = 29 um.

Fig45

Fig.46 HAG, 2 weeks after lesion. The presence of autofluorescent cells is consistently observed (arrowheads) at the lesion area. Bar = 29 um.

Fig46

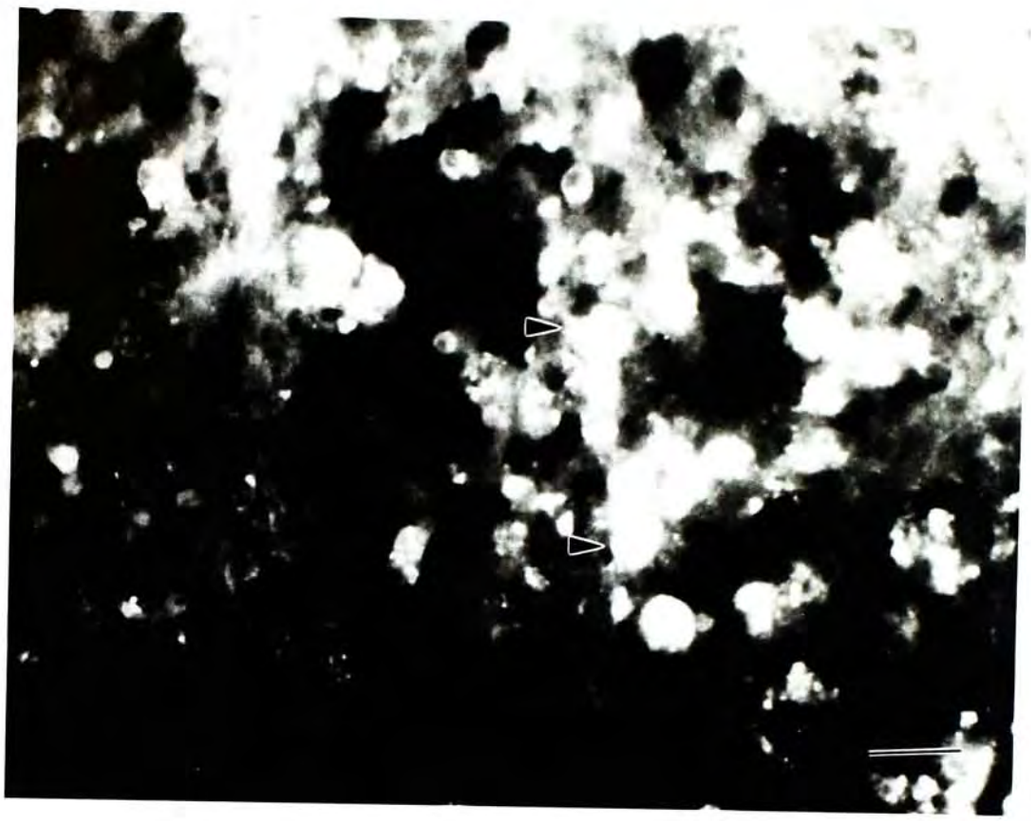

Fig.47 HG, 1 month after surgery. Fibroblast containing dilated rough endoplasmic reticulum (arrowheads), is found interpersed among collagen fibres (C). Bar = 0.8 um.

Fig.48 HAG, 1 month after surgery. Fibroblast with expanded rough endoplasmic reticulum (arrowheads) in the lesion site. Bar = 0.5 um.

Fig47and48

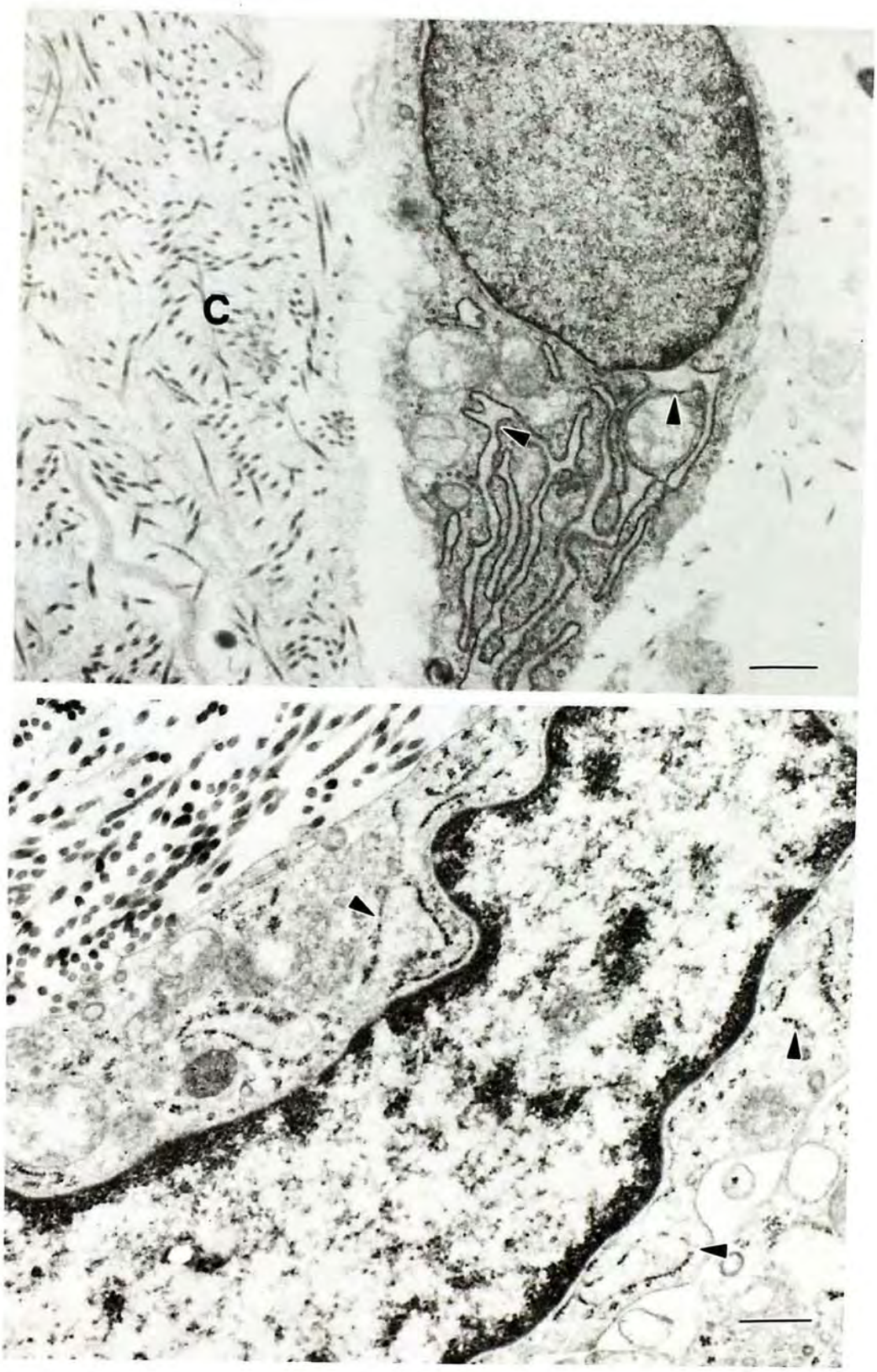

Fig.49 HG, 1 month after lesion. Macrophage containing lysosomes engulfs gelfoam (arrowheads). Bar = 0.8 um.

Fig.50 HAG, 1 month after lesion. Phagocyte located near gelfoam (arrowhead), with several lysosomes contained in the cytoplasm. Bar = 1.5 um.

Fig 49 and 50

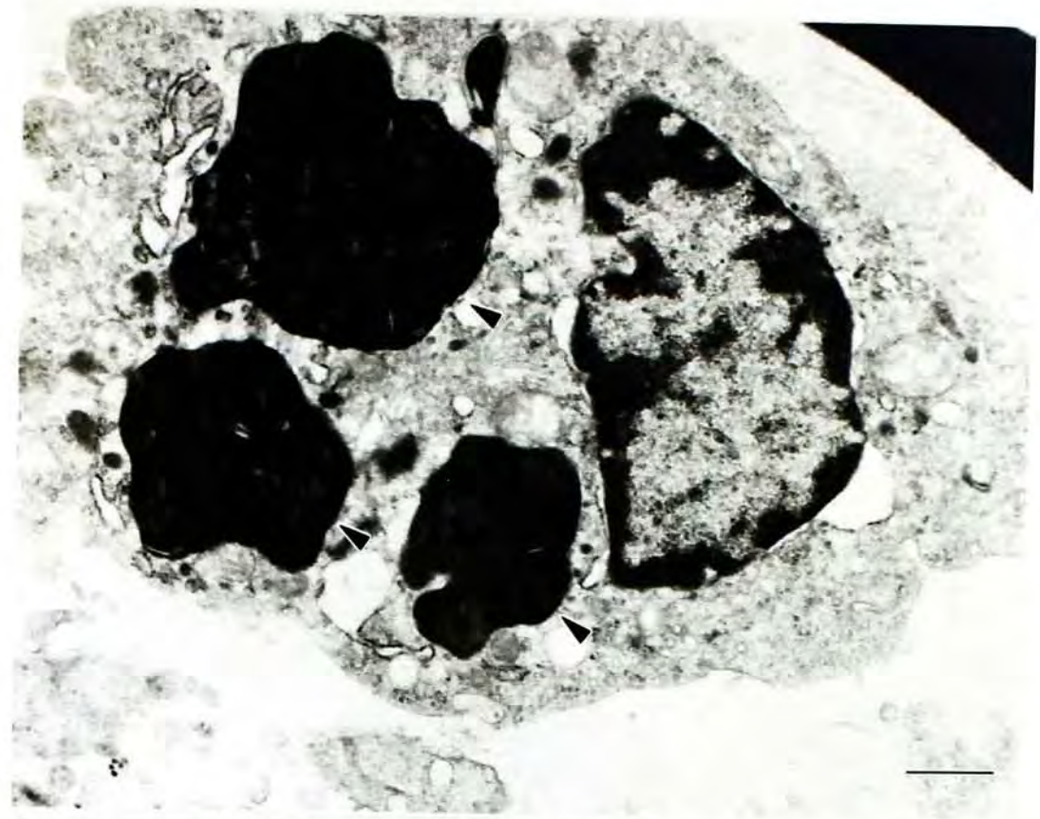

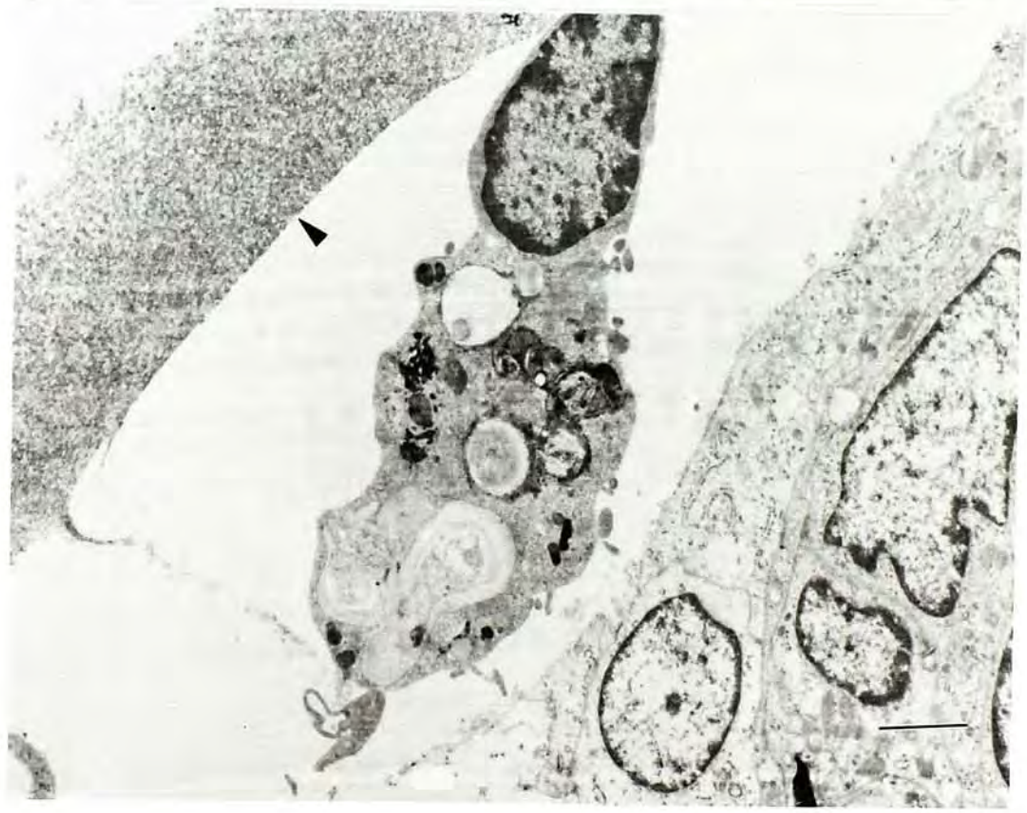

Fig.51 HG, 1 month after operation. Bundle of neurites (N) is accompanied by neuroglial cell (G). Bar = 0.4 um.

Fig 51

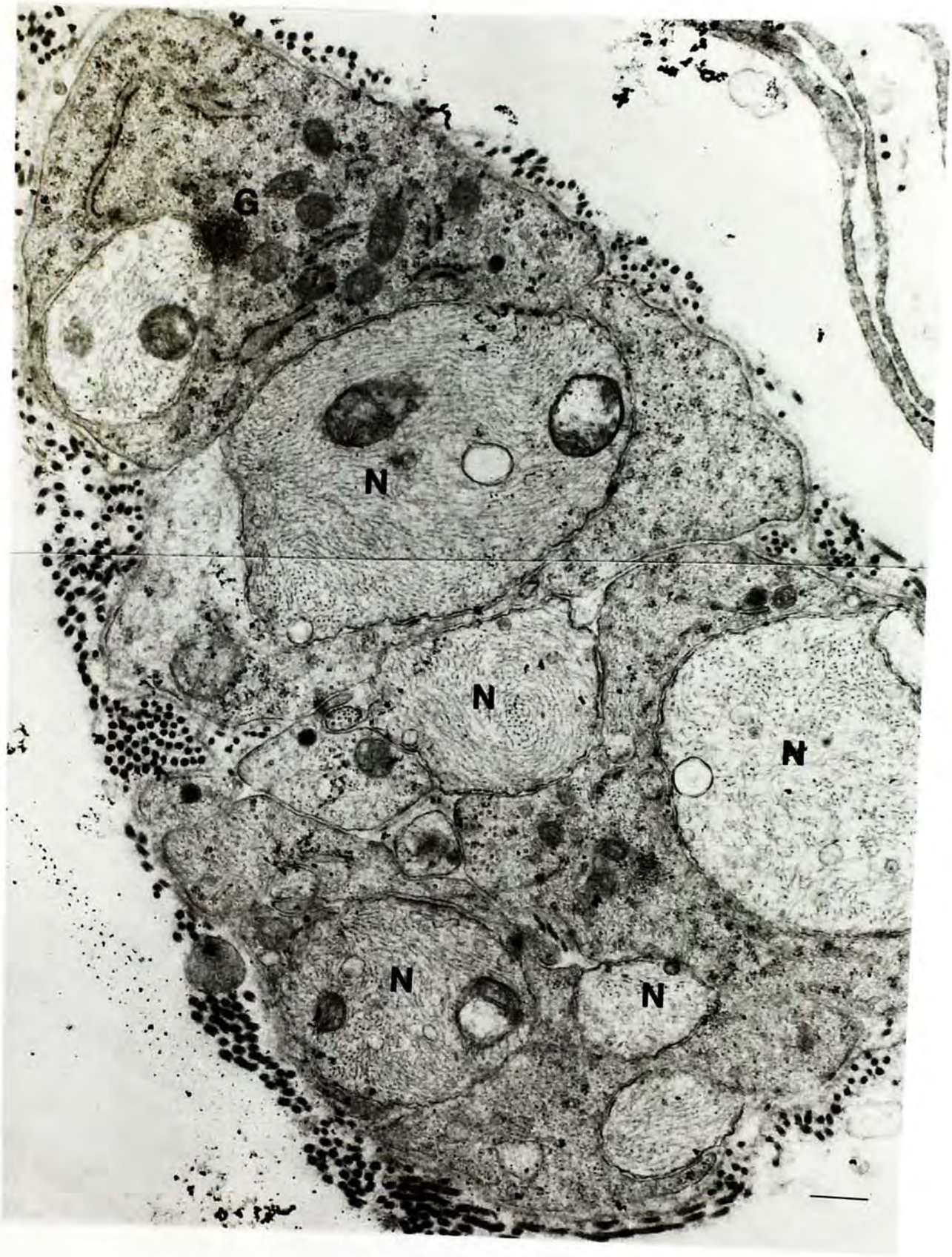

Fig.52 HAG, 1 month after operation. Clusters of myelinated axons (M) are interspersed with unmyelinated axons (U) in the lesion area. Bar = 0.4 um.

Fig.53 HAG, 1 month after operation. Blood vessels (b) are visible at the vicinity of myelinated axons (M). Bar = 0.8 um.

Fig.54 HAG, 1 month after operation. Electron dense region (arrowheads) is present between two apposing processes containing vesicles. Bar = 0.1 um.

Fig 52, 53 and 54

Fig.55 HAG, 2 months post surgery. In the lesion site, there are unmyelinated fibres containing microtubules (arrowhead) while neurites (n) possess numerous neurofilaments. M represents myelinated fibres. Bar = 0.5 um.

Fig.56 HAG, 2 months post surgery. Arrowhead indicates synapse. Bar = 0.9 um.

Fig.57 HG, 2 months post surgery. In the lesion site, myelinated fibres (M) are observed and some of them are abnormal (arrowheads). Bar = 0.9 um.

Fig55, 56 and57

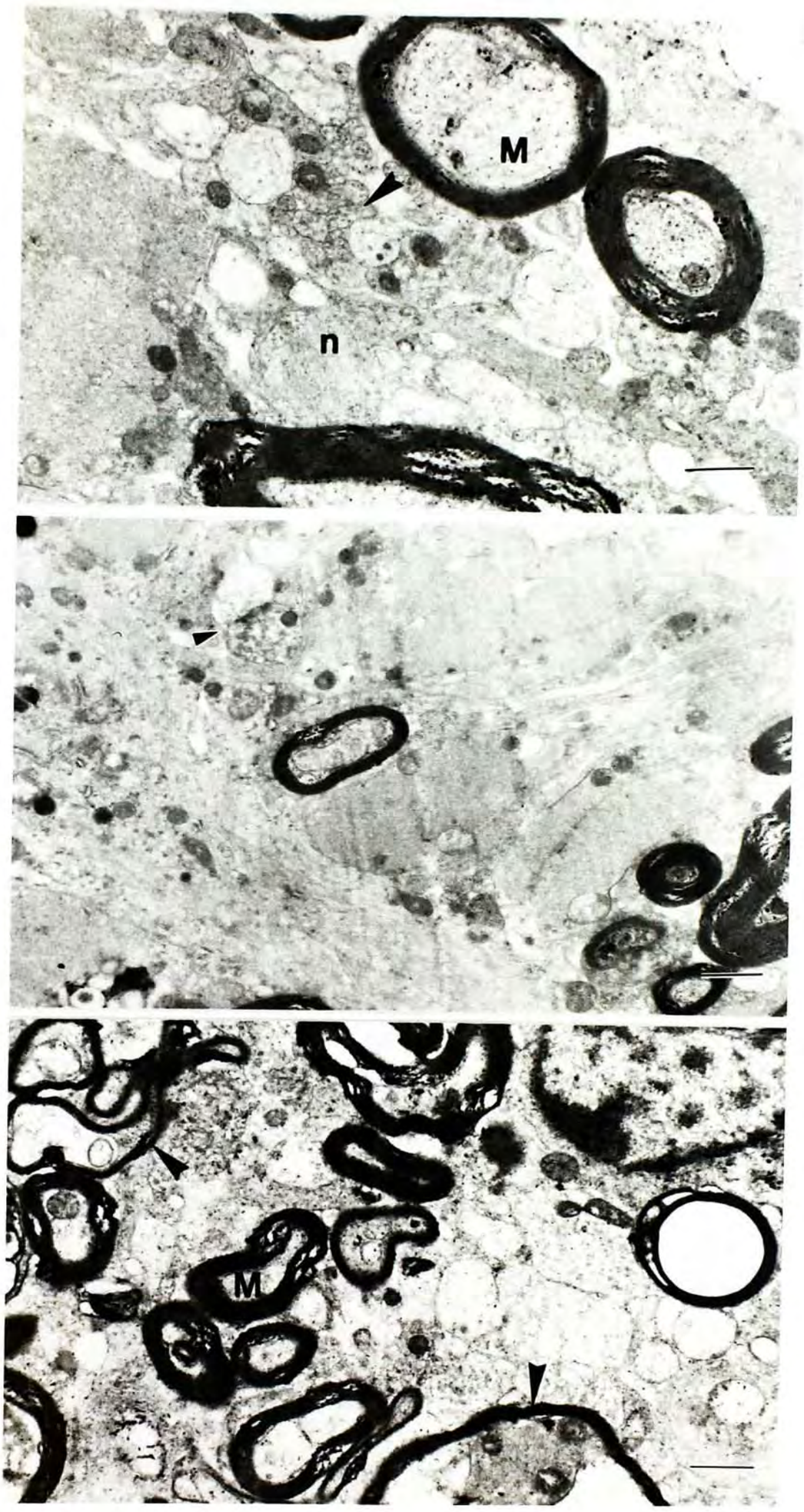

Fig.58HAG, 2 months after lesion. Nerve fibres (n) with synapses (arrows) are more numerous in region caudal to lesion. Myelinated fibres (M) are also observed. Bar = 0.5 um.

Fig.59HG, 2 months after lesion. Lots of abnormal looking myelinated axons (M) are present in region caudal to lesion. Bar = 0.5 um.

Fig 58and59

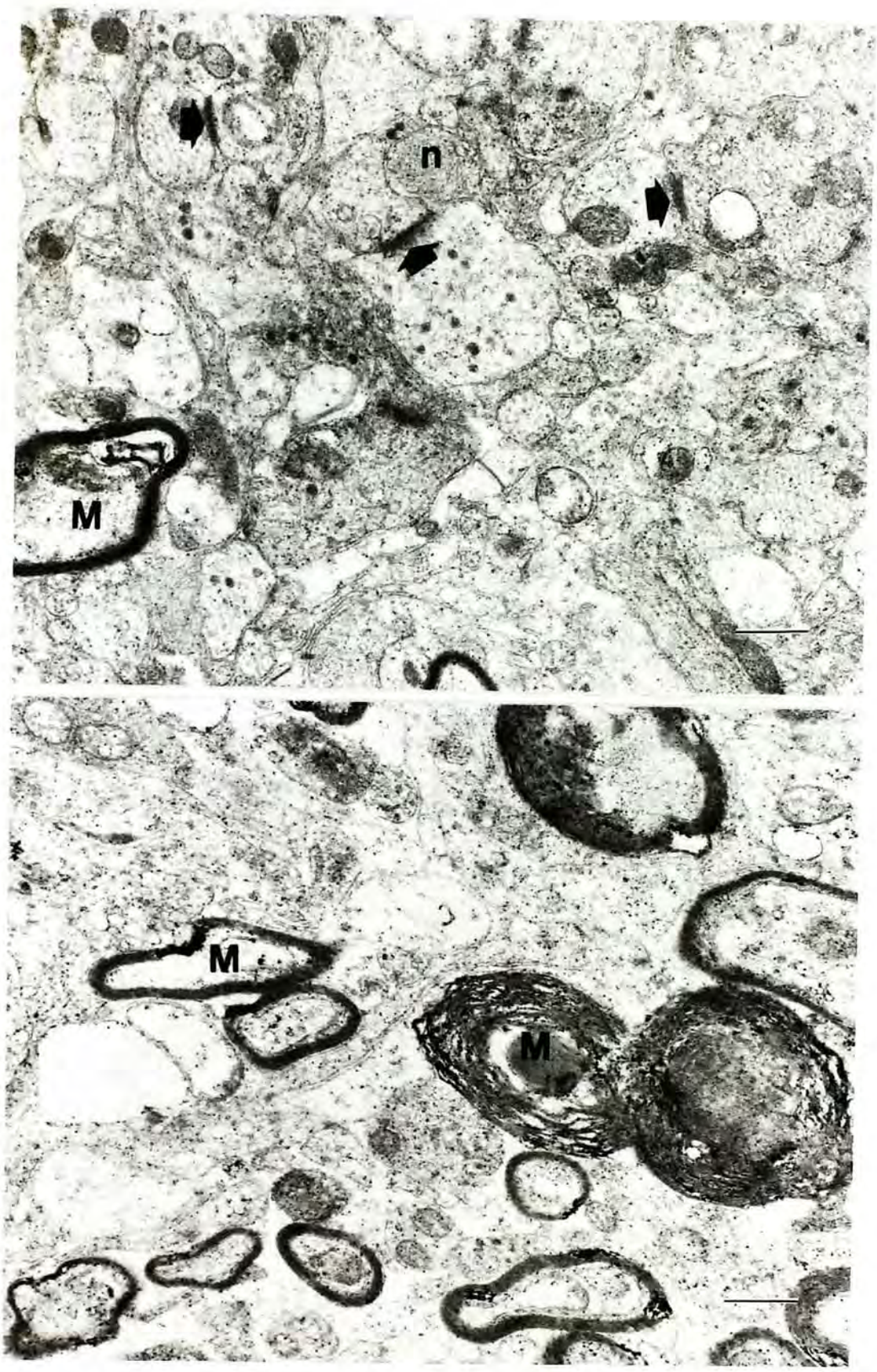

Fig 60

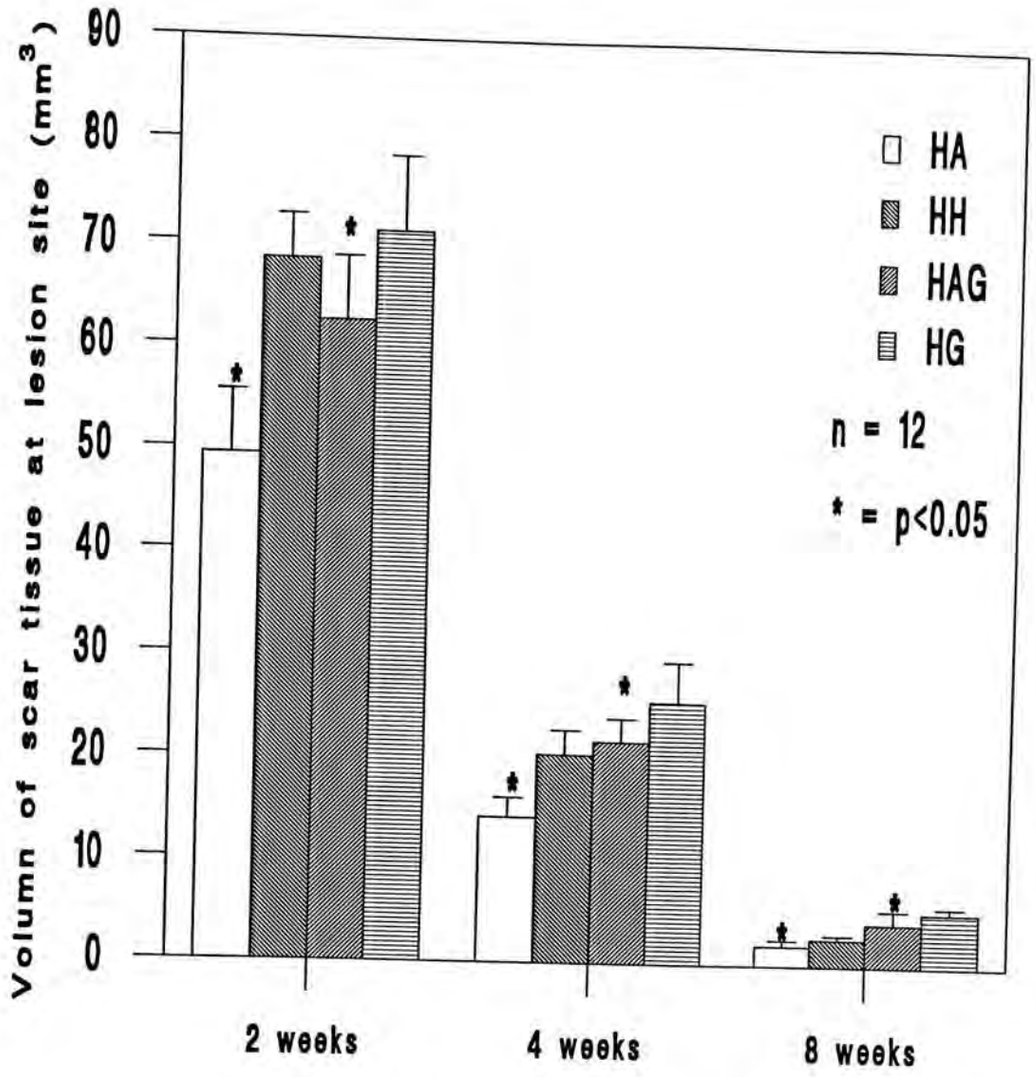

Change in the volume of spinal cord scar tissue in the experimental (HA and HAG) and control (HH and HG) groups from 2 weeks to 2 months after surgery

Fig.61Lane 1: molecular weight standards (49,000 - 205,000 daltons); Lane 2: phosphate buffer; Lane 3: suspension from intact spinal cord.

Fig.62HA and HH gel electrophoresis 2 months after surgery. Lane 0 and 9: phosphate buffer. Lane 1 and 8: molecular weight standards (49,000 - 205,000); Lane 2, 3, 4: HH group; Lane 5, 6, 7: HA group. a: MW = 180 kd. b: MW = 130 kd. c: MW = 80 kd. d: MW = 35 kd.

Distribution of the protein bands from the HA and HH groups is similar to that from the intact spinal cord.

Fig 61 and 62

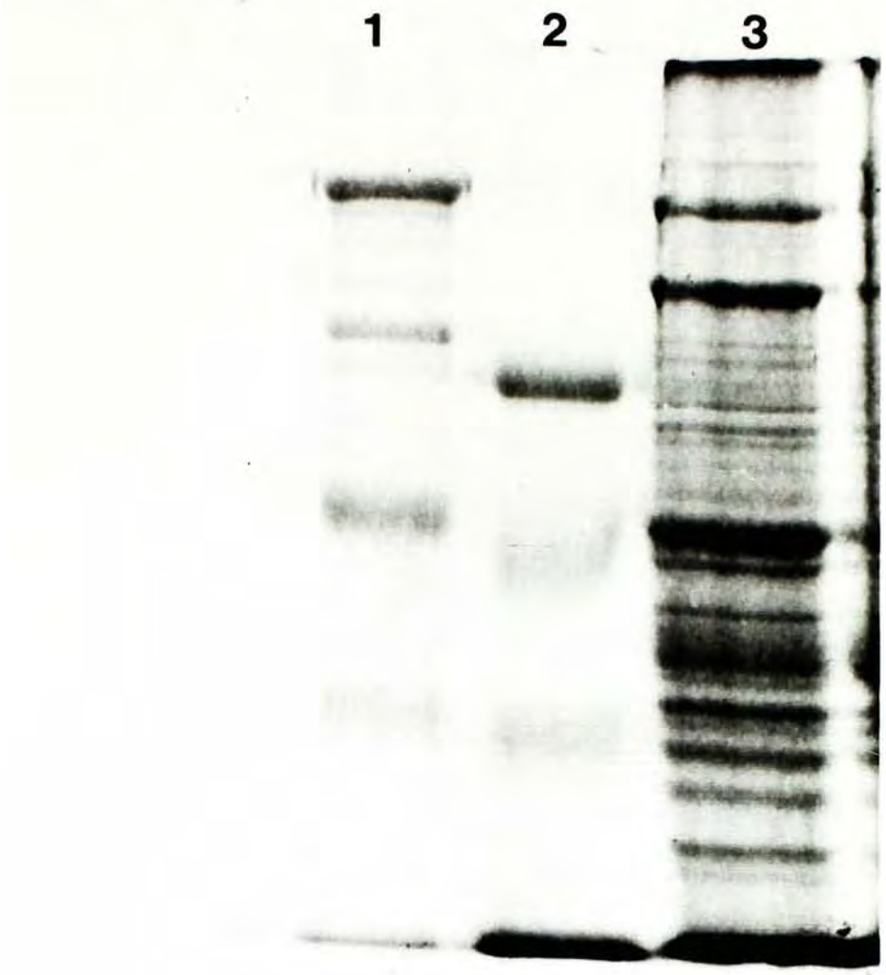

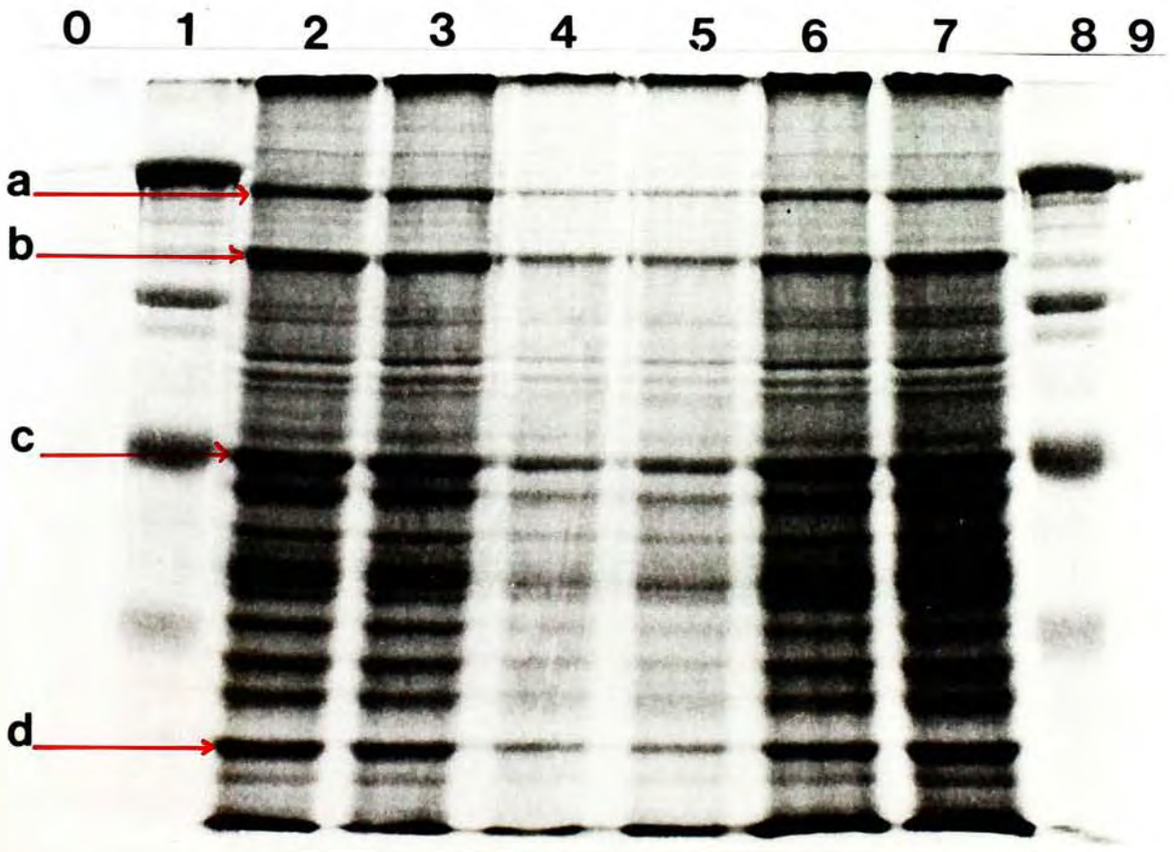

Fig.63 Immunoblotting in HA and HH 2 months after lesion. Lane 1 and 8: molecular weight standards (49,000 - 205,000 daltons); Lane 2 : HA, without primary antibody to GFAP; Lane 3: HA, GFAP staining (arrowhead); Lane 4 and 5: phosphate buffer; Lane 6: HH, GFAP staining (arrowhead); Lane 7: HH, without primary antibody to GFAP.
There is a comparatively lower quantity of GFAP in the HA group.

Fig.66 Immunoblotting for NF 68 and 160 kd in HA and HH 2 months after lesion. Lane 1 and 10: phosphate buffer; Lane 2 and 9: molecular weight standards (49,000 - 205,000 daltons); Lane 3: HA, NF 160 kd (arrowhead); Lane 4: HA, NF 68 kd (arrowhead); Lane 5 and 6: mouse ascites fluid; Lane 7: HH, NF 68 kd (arrowhead); Lane 8: HH, NF 160 kd (arrowhead). Darker and broader bands of both NF 68 kd and 160 kd are found in the HA group, compared with that in the HH group.

Fig63

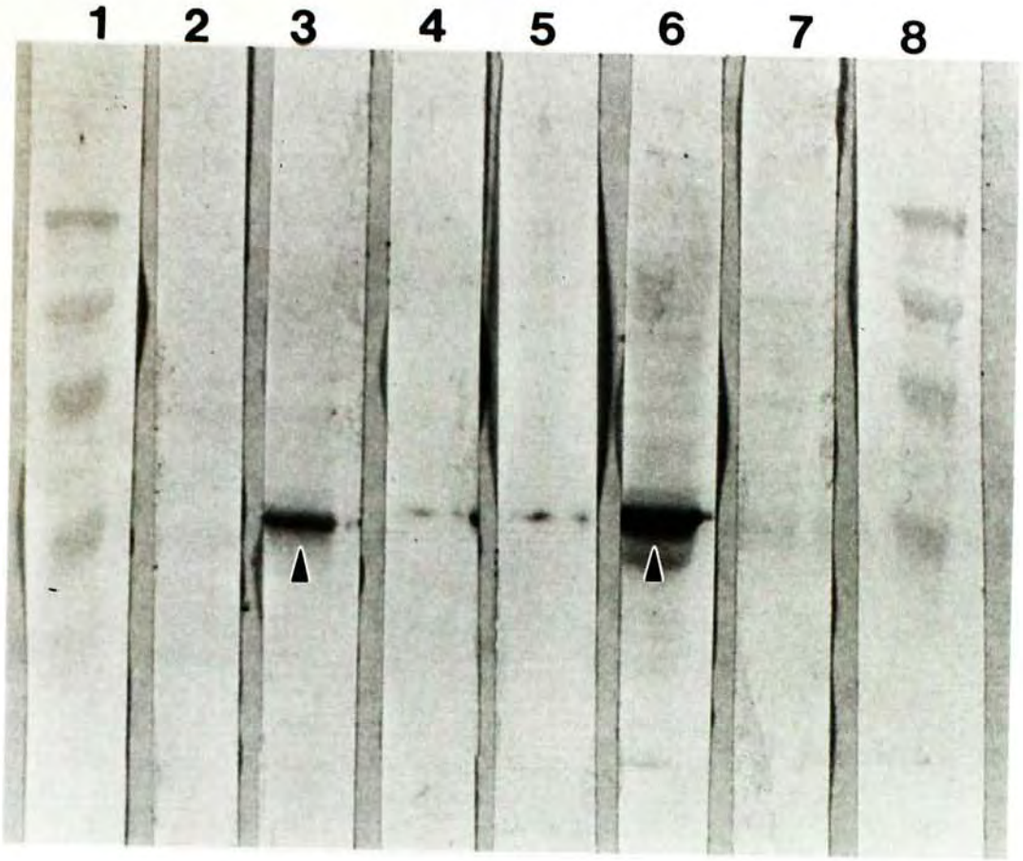

Fig66

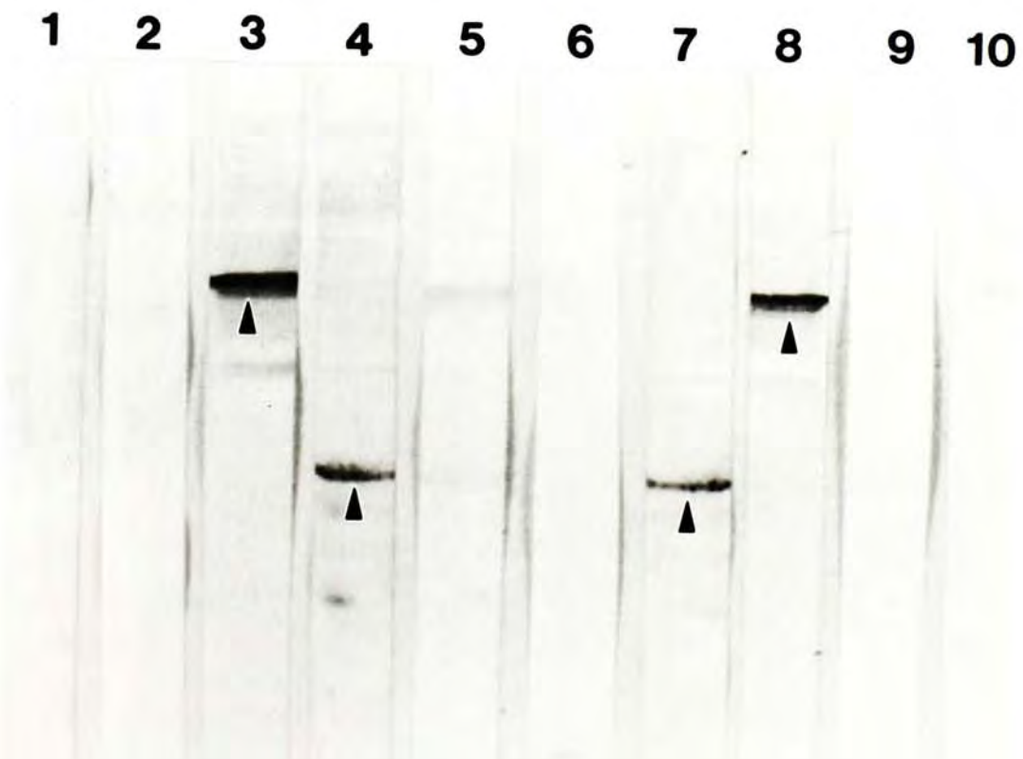

Fig 64 Densitometry tracing of GFAP in the HA group.

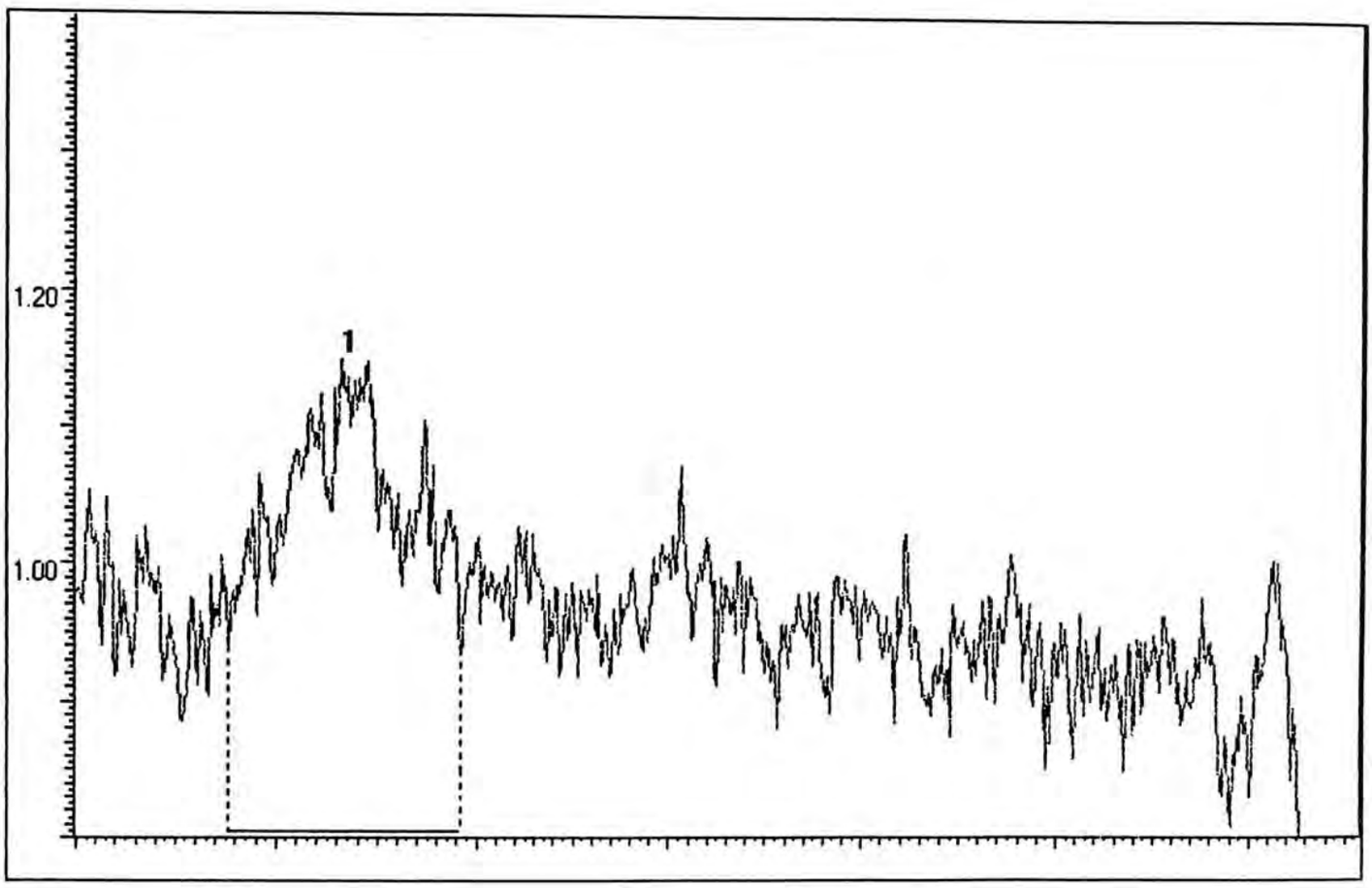

Peak pixel value: 1.304; Volume: 13.96

Fig 65 Densitometry tracing of GFAP in the HH group.

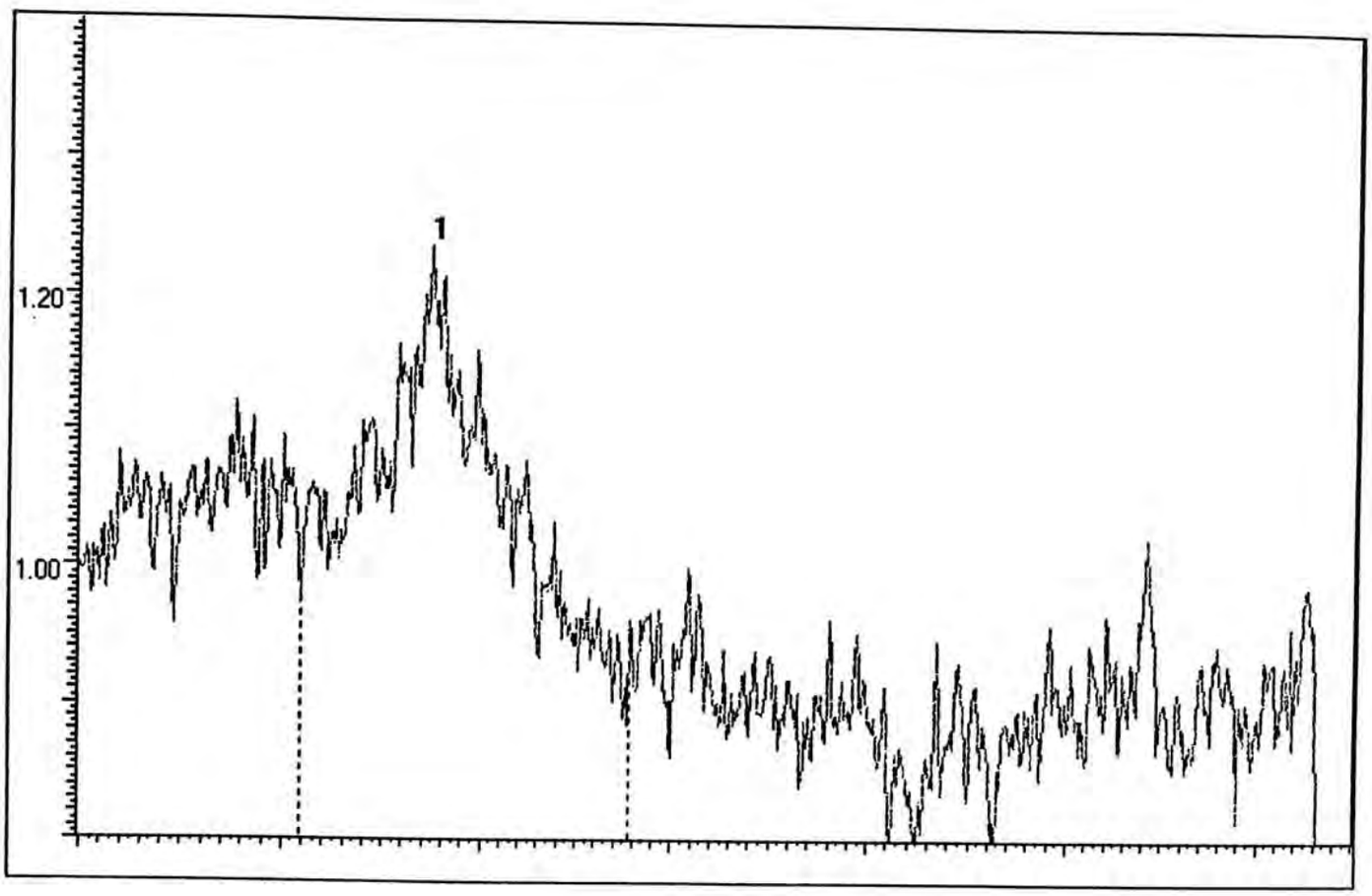

Peak pixel value: 1.403; Volume: 38.05

Fig67 Densitometry tracing of NF 68 in the HA group.

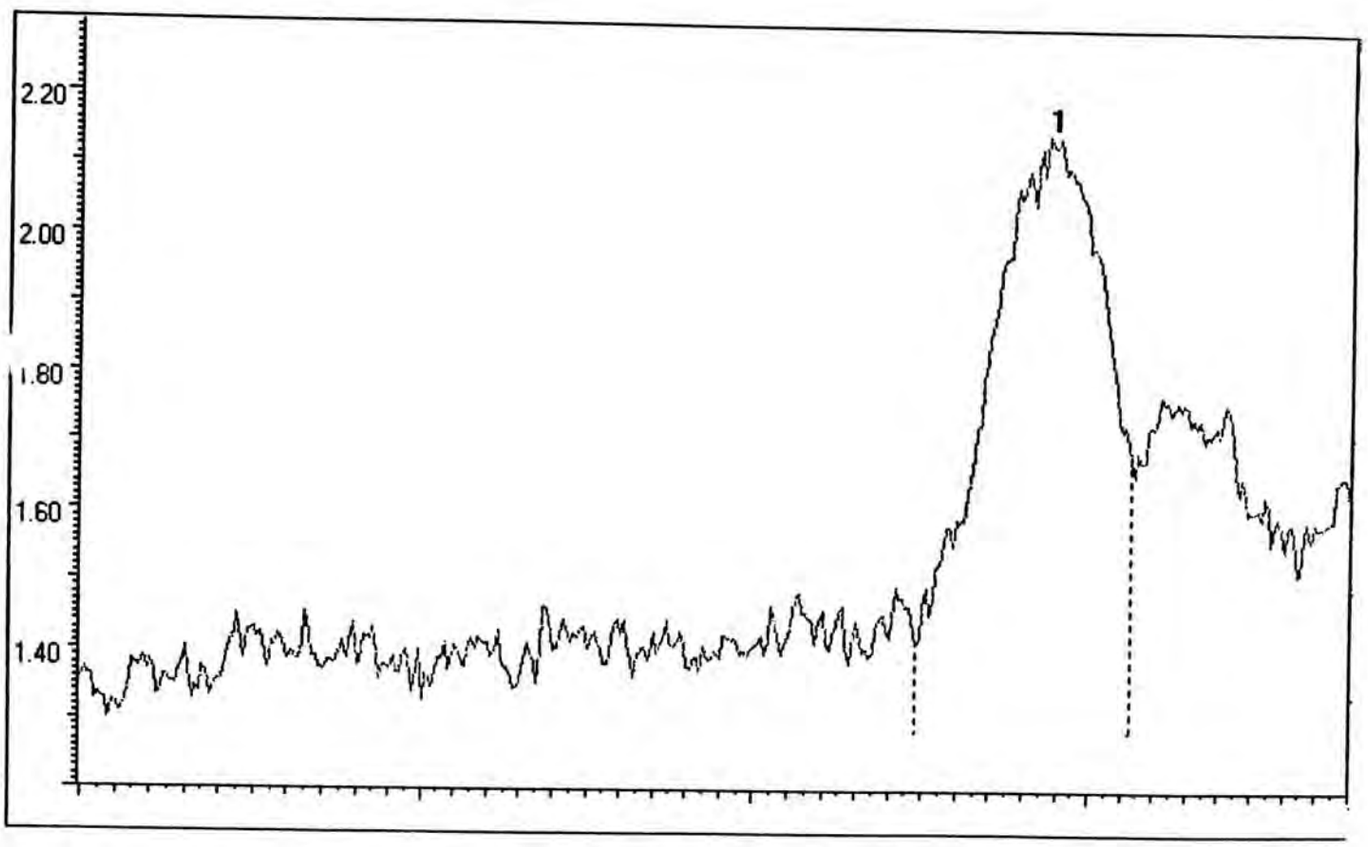

Peak pixel value: 2.182; Volume: 36.22

Fig68 Densitometry tracing of NF 68 in the HH group.

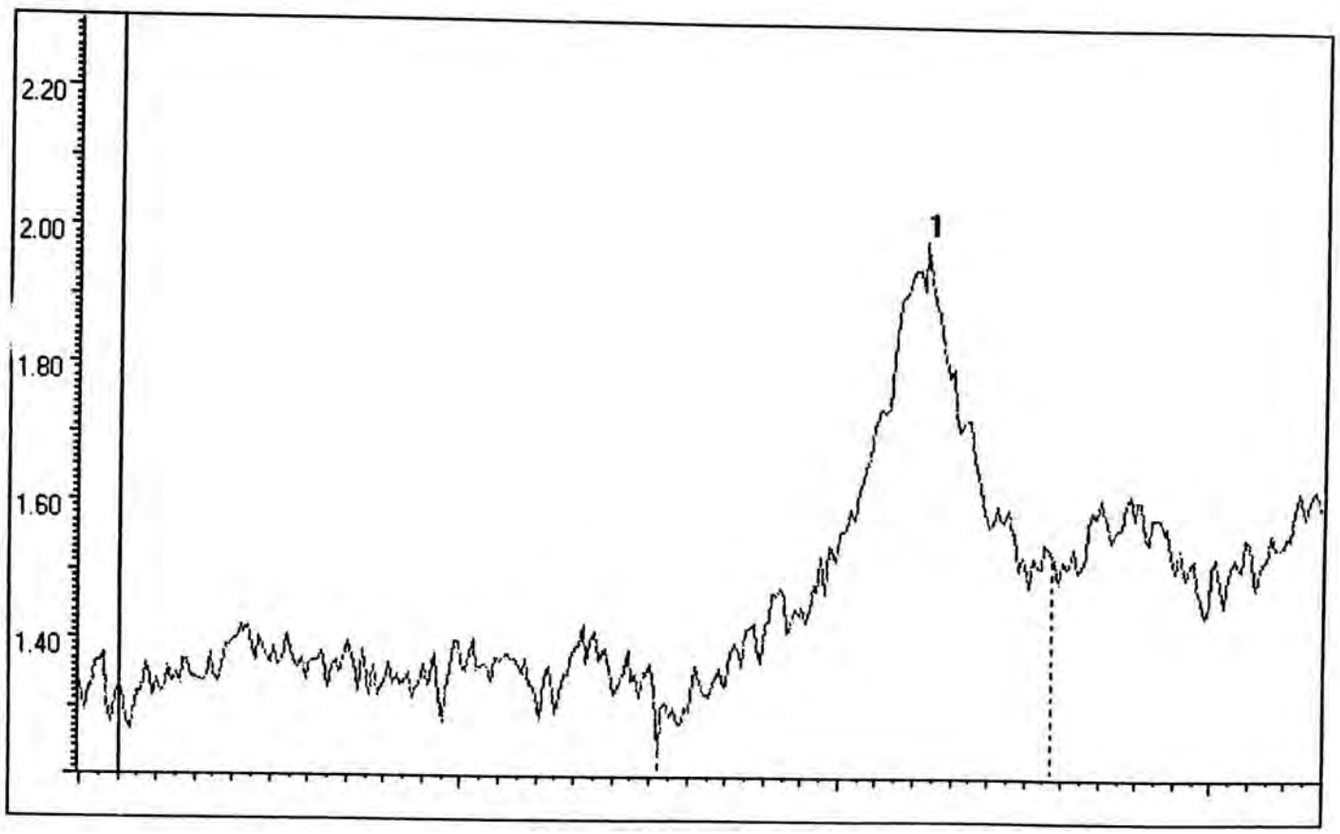

Peak pixel value: 1.982; Volume: 23.39

Fig69 Densitometry tracing of NF 160 in the HA group.

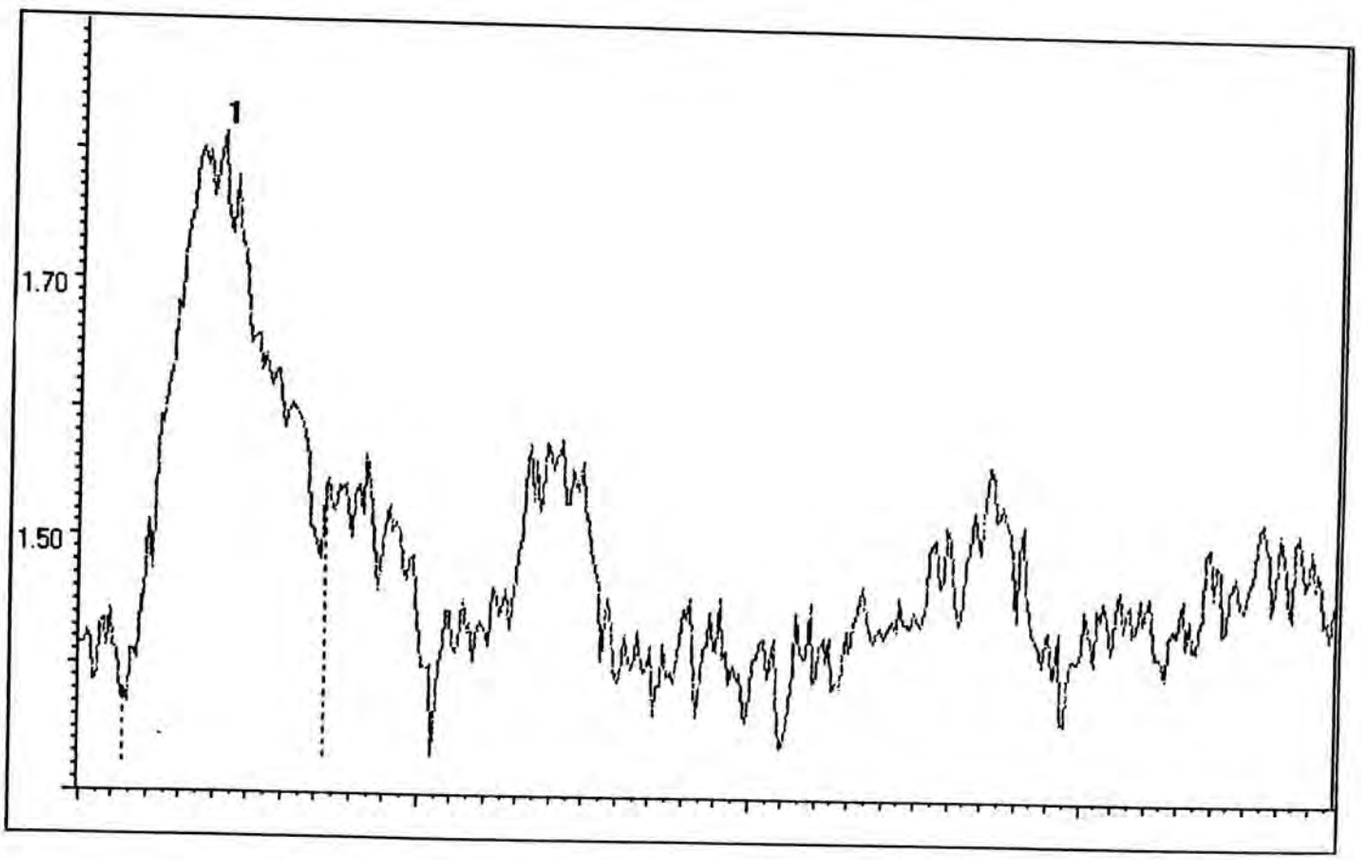

Peak pixel value: 1.807; Volume: 17.59

Fig70 Densitometry tracing of NF 160 in the HH group.

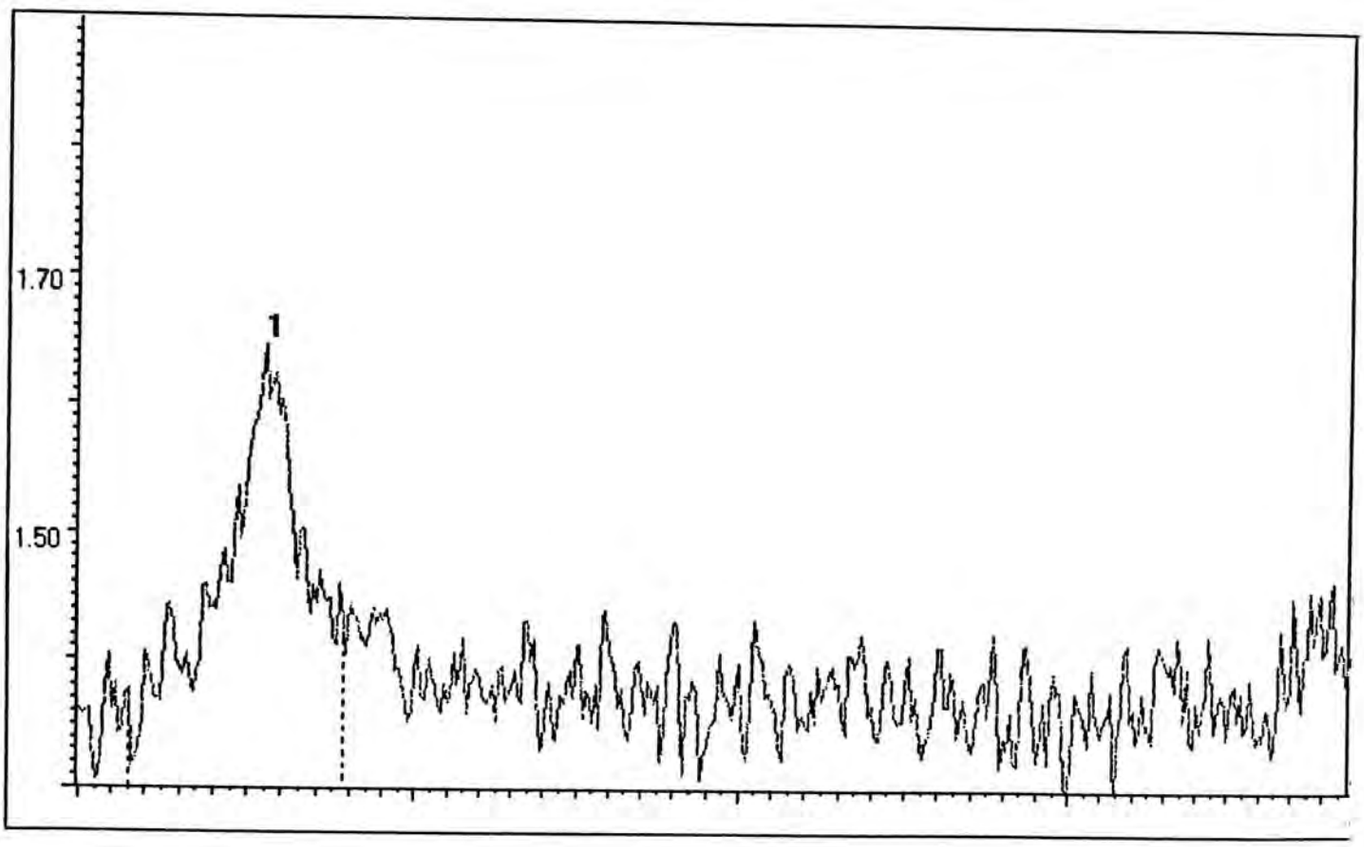

Peak pixel value: 1.667; Volume: 14.15

Table 1. Morphological observations on the H & E Staining in the experimental (HA and HAG) and control (HH and HG) groups from 2 weeks to 2 months after surgery

	HA	HH	HAG	HG
Tissue necrosis	Most prominent in 2 weeks, reduced over time	More extensive than HA in all survival periods	Most prominent in 2 weeks, reduced over time	More extensive than HAG in all survival periods
Macro-phages	Number of macrophages decreased with time	Considerably more macrophages than HA, decreased with time	Number of macrophages decreased with time	Slightly more macrophages than HAG; Number decreased with time
Gliosis	Number of astrocytes decreased; More collagen-like fibres at 1 and 2 months	More numerous glial cells than in HA; Number decreased with time	Gliosis decreased with time at a greater extent than HG	Gliosis decreased with time
Blood vessels	Scarce at 2 weeks; More numerous at 1 month after lesion	Very few blood vessels	Very few blood vessels	Very few blood vessels
Nerve-like fibres	Organized into bundles and extended into lesion site observed as early as 2 weeks after lesion	Nerve-like fibres rarely observed	More numerous well-organized nerve-like fibres especially at 2 months after lesion	Nerve-like fibres were disorganized

IV. Discussion and conclusions

This study has studied the histological and biochemical response of the adult rat spinal cord from 2 weeks to 2 months following hemisection. Rats in the experimental groups had cultured astrocytes introduced into the lesion site either in the form of suspension injection (HA) or they were first cultured on gelfoam and implanted (HAG). In all rats, experimental and control, morphological observations showed that following lesion there was degeneration of neuronal tissues accompanied by the infiltration of phagocytes. Cystic cavities formed and astrogliosis followed soon after. However, it was noted histologically that the experimental groups appeared to undergo less massive degeneration and astrocytic gliosis. This was confirmed by (1) the volume measurements which showed that the amount of scar tissue in the experimental groups was always less than that of the control at all time points; (2) the western blotting which demonstrated reduced GFAP in the experimental group (HA). Immunofluorescence staining showed that neurites were present as early as 2 weeks after lesion. Their presence was confirmed by ultrastructural observations which demonstrated that synapses could be found in the experimental group (HAG) 2 months after lesion. Synapses were not as easily observed in the control group (HG). Results of western blotting showed increased expression of NF 68 and 160 in the experimental group (HA), suggesting that there were more nerve fibres present.

One of the findings in this study is that tissue scarring in experimental animals was consistently less than that of control and the discrepancy was already apparent 2 weeks after lesion. The similar rate of scar reduction in all groups suggests that the implanted cultured astrocytes probably had little direct effect in promoting recovery of injured tissue over a prolonged period. This notion is supported also by the finding that the implanted astrocytes migrated quite extensively in the SC, at a rate of about 0.6mm/day. The rate is quite similar with that obtained by Goldberg and Bernstein (1988) who showed that PHAL-labelled astrocytes migrated at a rate of about 0.72mm/day in the adult rat thoracic spinal cord. The results thus suggest that the effect of the implanted astrocytes probably occurs over a short time course, perhaps within a few days, soon after introduction into the lesion site. Its influence over this short period of time, however, is sufficient to result in the decreased tissue scarring observed at two weeks post lesion.

Evidence from several previous studies do indeed strongly indicate that this is the case (e.g. Ferrara et al., 1988; Giulian et al., 1988, 1993). Previous studies have shown that astrocytes and microglia which are stimulated to become phagocytes during injury (Giulian, 1987) release factors which act on each other as well as neighbouring neurons. It is within the first week of spinal cord injury that there is maximal infiltration of phagocytes and removal of cell debris (Curtis et al., 1993). Astrocytes

produce neurotrophic factors such as basic fibroblast growth factor (bFGF) and ciliary neurotrophic factor (CNTF) (Ferrara et al., 1988; Rudge et al., 1985) while microglia produce a variety of cytokines and degradative enzymes (North, 1978). In addition to producing substances with opposing actions, they also secrete mitogens to stimulate each others' division (Giulian and Ingeman, 1988). However, inspite of these divergent effects, a recent study has shown that astrocyte-released factors if present at a sufficiently high concentration, can counteract the neurotoxic effects of microglia (Vaca and Wendt, 1992). It is possible that in this study the implanted astrocytes played a positive role in counteracting the deleterious effects of microglia and thus reduced the amount of degeneration and scarring.

It should be noted that not all the secretions produced by microglia may be interpreted as inhibitory to neurite growth. Interleukin 1, which is produced by microglia and cultured astrocytes (Giulian, 1987) has been shown to promote neovascularization (Giulian et al., 1988). This could well be significant in neuronal recovery because in this study the presence of blood vessels was consistently found in the HA group as verified by routine light microscopy and immunofluorescence. The immunofluorescence staining also demonstrated the presence of N-CAM on the periphery of these blood vessels; N-CAM is well known as a neurite promoting molecule (e.g. Neugebauer et al., 1988; Persohn et al., 1987). At the same time ultrastructural observations

showed that axons, particularly myelinated ones, were found in the vicinity of blood vessels. Taking together these findings, it is tempting to speculate whether the implanted astrocytes may have contributed to the neovascularization and hence indirectly helped in neurite growth. Interestingly, in a recent study Curtis and his colleagues (1993) found that early axonal elongation following SC compression was also preferentially associated with newly formed capillaries.

Transmission electron microscopy and immunofluorescence staining for neurofilaments demonstrated that most of the neurite growth was found in a region of the SC caudal to the lesion. It is likely that these neurites are ascending sensory fibers which are attempting to regenerate. Support for this notion can be found in the results of a study by Martin et al (1991). They demonstrated that cultured Schwann cells implanted into a compression lesion of the adult rat SC promoted axonal regrowth mostly from dorsal root ganglion cells, not from descending fibres. It could be that sensory fibres intrinsically have a greater potential to regenerate than descending motor fibres. On the other hand, one cannot rule out the possibility that the preferred caudal migratory route of introduced astrocytes can alter the microenvironment such that the region of the SC immediately caudal to the lesion becomes more permissive to neurite growth.

Immunofluorescence staining for N-CAM in this study showed that there was some reinduction of N-CAM expression in the region

around the lesion with slightly more staining in the experimental groups. This finding agrees with previous reports which showed that regenerating sciatic nerves increase their expression of N-CAM (Martini and Schachner, 1988).

The secretion of neurotrophic factors from cultured astrocytes and their ability to promote neurite growth has been well documented in previous in vitro studies (Rudge et al., 1985; Ferrara et al., 1988; Martin, 1992). Furthermore, Geisert and Stewart (1991) found that astrocytes purified from neonatal rat cortex elicited longer neurites from neurons than those purified from the adult rat cortex. These in vitro studies show a direct neurotrophic effect of the cultured astrocytes. Although this study has utilized astrocytes cultured from neonatal rat cortex, it is uncertain whether the relative increased neurite growth in the experimental rats can be directly attributed to the neurotrophic effect of the implanted astrocytes. One major reason for this doubt is the finding that the implanted astrocytes migrated both from the original site of injection and also the gelfoam. Perhaps a more convincing explanation is that the experimental rats had less tissue scarring, evident as early as 2 weeks post lesion (cf III.4), and this represents less of a barrier to neurite growth. Hence an important subject for further investigation would be the effect of the cultured astrocytes in the lesion site within the first two weeks following lesion.

In conclusion, the results of this study indicate that there

is some therapeutic value in implanting cultured astrocytes in hemisected adult rat SC as evidenced by the decreased tissue scarring and increased nerve fibre growth in the experimental rats. An advantage in using cultured astrocytes is that the cells can be produced easily in large quantities. However, it is uncertain whether these cells retain their original properties as in the in vitro state, or if they are able to survive for long periods. Further investigation is needed to address these questions. Also, future studies could look into the cellular interaction between the implanted astrocytes and other cells in the SC, particularly in the first week following hemisection.

REFERENCES

Adrian, E.K., and Willians, M.G. (1973). Cell proliferation in injured spinal cord. An electron microscopic study. J. Comp. Neurol. 151, 1-24.

Adrian, E.K., Williams, M.G., and George, F.C. (1978). Fine structure of reactive cells in injured nervous tissue labelled with ^{3}H-thymidine injected before injury. J. Comp. Neurol. 180, 815-840.

Anderson, P.N., Mitchell, J., Mayor, D., and Stauber, V.V. (1983). An ultrastructural study of the early stages of axonal regeneration through rat nerve grafts. Neuropathol. Appl. Neurobiol. 9, 455-466.

Arteta, J.L. (1956). Research on the regeneration of the spinal cord in the cat submitted to the action of pyrogenous substances of bacterial origin. J. Comp. Neurol. 105, 171-184.

Baird, A., and Walicke, P.A. (1989). Fibroblast growth factors. Brit. Med. Bull. 45, 438-452.

Barr, M.L., and Hamilton, J.D. (1948). A quantitative study of certain morphological changes in spinal motor neurons during axon reaction. J. Comp. Neurol. 89, 93-112.

Barron, K.D., and Doolin, P.F. (1969). Neuronal responses to axonal injury. In: Contemporary Neurol. Vol. II, (F.H. Norris and L.Kurland eds), pp. 301-318, Grune and Stratton, New York.

Bernstein, J.J., and Bernstein, M.E.(1969). Ultrastructure of

normal regeneration and loss of regenerative capacity following teflon blockage in goldfish spinal cord. Exp. Neurol. 24, 538-557.

Bernstein, J.J., and Bernstein, M.E. (1971). Axonal regeneration and formation of synapses proximal to the site of lesion following hemisection of the rat spinal cord. Exp. Neurol. 30, 336-351.

Bernstein, J.J., Patel., U., Kelemen, M., Jefferson, M., and Turtil, S. (1984). Ultrastructure of fetal spinal cord and cortex implants into adult rat spinal cord. J. Neurosci. Res. 11, 359-372.

Berry, M., and Riches, A.C. (1974). An immunological approach to regeneration in the central nervous system. Br. Med. Bull. 30, 135-140.

Berry, M. (1979). Regeneration in the central nervous system. In: Recent advances in neuropathology, Vol.1, (W.T. Smith (ed.), pp. 67-111, Churchill Livingstone, Edinburgh.

Berry, M., Rees, L., Hall, S., Yiu, P., and Sievers, J. (1988). Optic axons regenerate into sciatic nerve isografts only in the presence of Schwann cells. Brain Res. Bull. 20, 223-231.

Bjerre, B., Bjorklund, A., and Stenevi, U. (1973). Stimulation of growth of new axonal sprouts from lesioned monoamine neurons in adult rat brain by nerve growth factor. Brain Res. 60, 161-176.

Bjerre, B., Bjorklund, A., and Stenevi, U. (1974). Inhibition of

the regenerative growth of central noradrenergic neurons by intracerebrally administered anti-NGF serum. Brain Res. 74, 1-18.

Blakemore, W.F. (1983). Remyelination of demyelinated spinal cord axons by Schwann cells. In: Spinal Cord Reconstruction (C.C. Kao, R.P. Bunge, and P.J. Reier eds.), pp. 281-291, Raven Press.

Bovolenta, P., Wandosell, F., and Nieto-Sampedro, M. (1991). Neurite outgrowth over resting and reactive astrocytes. Restor. Neurol. and Neurosci. 2, 221-228.

Cajal, S. Ramon y (1928). Degeneration and Regeneration of the nervous system. Translated by R.M. May. Hafner, New York.

Carden, M.J., Trojanowski, J.Q., Schlaepfer, W.W., and Lee, V.M.-Y. (1987). Two-stage expression of neurofilament polypeptides during rat neurogenesis with early establishment of adult phosphorylation patterns. J. Neurosci. 7, 3489-3504.

Chambers, W.W. (1955). Structural regeneration in the mammalian central nervous system. pp. 135-146, Thomas, Springfield.

Chiu, A.Y., De Los Monteros, A., Cole, R.A., Loera, S., and De Vellis, J. (1991). Laminin and s-Laminin are produced and released by astrocytes, Schwann cells, and Schwannomas in culture. Glia 4, 11-24.

Chuong, C.M., and Edelman, G.M. (1984). Alterations in neural cell adhesion molecules during development of different regions of the nervous system. J. Neurosci. 4, 2354-2368.

Clark, L.G. (1943). Axonal regeneration in the mammalian central nervous system. (D.E. Oorschot and D.G. Jones eds.), pp. 6-14, Springer-Verlag.

Clemente, C.D. (1964). Regeneration in the vertebrate central nervous system. Int. Rev. Neurobiol. 6, 257-301.

Curtis, R., Green, D., Lindsay, R.M., and Wilkin, G.P. (1993). Up-regulation of GAP-43 and growth of axons in rat spinal cord after compression injury. J. Neurocytol. 22, 51-64.

Edelman, G.M. (1985). Cell adhesion and the molecular processes of morphogenesis. Annu. Rev. Biochem. 54, 135-169.

Edelman, G.M. (1988). Morphoregulatory molecules. Biochem. 27, 3533-3543.

Egan, D.A., Flumerfelt, B.A., and Gwyn, D.G. (1977). A light and electron microscopic study of axon reaction in the red nucleus of the rat following cervical and thoracic lesions. Neuropathol. Appl. Neurobiol. 3, 423-439.

Egan, D.A., Flumerfelt, B.A., and Gwyn, D.G. (1977). Axon reaction in the red nucleus of the rat. Acta Neuropathol. (Berl.). 37, 13-19.

Feringa, E.R., Gurden, G.G., Strodel, W., Chandler, W., and Knake, J. (1973). Descending spinal motor tract regeneration after spinal cord transection. Neurol. 23, 599-608.

Feringa, E.R., Kowalski, T.F., and Vahlsing, H.L. (1980). Basal lamina formation at the site of spinal cord transection. Ann. Neurol. 8, 148-154.

Ferrara, N., Ousley, F., and Gospodarowicz, D. (1988). Bovine brain astrocytes express basic fibroblast growth facor, a neurotropic and angiogenic mitogen. Brain Res. 462, 223-232.

Figlewicz, D.A., Gremo, F., and Innocenti, G.M. (1988). Differential expression of neurofilament subunits in the developing corpus callosum. Dev. Brain Res. 42, 181-189.

Geisert, Jr., E.E., and Stewart, A.M. (1991). Changing interaction between astrocytes and neurons during CNS maturation. Dev. Biol. 143, 335-345.

Giulian, D. (1987). Ameboid microglia as effectors of inflammation in the central nervous system. J. Neurosci. Res. 18, 155-171.

Giulian, D., and Ingeman, J.M. (1988). Colony-stimulating factors as promoters of ameboid microglia. J. Neurosci. 8, 4707-4717.

Giulian, D., Vaca, K., and Johnson, B. (1988). Secreted peptides as regulators of neuron-glia and glia-glia interactions in the developing nervous system. J. Neurosci. Res. 21, 487-500.

Giulian, D., Vaca, K., and Corpuz, M. (1993). Brain glia release factors with opposing actions upon neuronal survival. J. Neurosci. 13, 29-37.

Glaze, K.A., and Turner, J.E. (1978). Regenerative repair in the severed optic nerve of the newt: effect of nerve growth factor antiserum. Exp. Neurol. 58, 500-510.

Goldberg, W.J., and Bernstein, J.J. (1988). Migration of cultured fetal spinal cord astrocytes into adult host cervical cord and medulla following transplantation into thoracic spinal cord.

J. Neurosci. Res. 19, 34-42.

Grafstein, B. (1975). The nerve cell body response to axotomy. Exp. Neurol. 48, 32-51.

Grant, G. (1985). Primary afferent projections to the spinal cord. In: The rat nervous system, (Paxinos, G. ed.), pp. 303-309, Academic Press.

Guth, L., Albuquerque, E.X., Deshpande, S.S., Barrett, C.P., Donati, E.J., and Warnick, J.E. (1980). Ineffectiveness of enzyme therapy on regeneration in the transected spinal cord of the rat. J. Neurosurg. 52, 73-86.

Guth, L., Barrett, C.P., Donati, E.J., Deshpande, S.S., and Albuquerque, E.X. (1981). Histopathological reactions and axonal regeneration in the transected spinal cord of hibernating squirrels. J. Comp. Neurol. 203, 297-308.

Guth, L., Reier, P.J., Barrett, C.P., and Donati, E.J. (1983). Repair of the mammalian spinal cord. Trends. Neurosci. 6, 20-24.

Hendry, I.A. (1975). The response of adrenergic neurons to axotomy and nerve growth factor. Brain Res. 94, 87-97.

Houle, J.D. (1991). Demonstration of the potential for chronically injured neurons to regenerate axons into intraspinal peripheral nerve grafts. Exp. Neurol. 113, 1-9.

Houle, J. (1992). The structural integrity of glial scar tissue associated with a chronic spinal cord lesion can be altered by transplanted fetal spinal cord tissue. J. Neurosci. Res. 31,

120-130.

Kao, C.C. (1974). Comparison of healing process in transected spinal cords grafted with autogenous brain tissue, sciatic nerve and nodose ganglion. Exp. Neurol. 44, 424-439.

Kiernan, J.A. (1978). An explanation of axonal regeneration in peripheral nerves and its failure in the central nervous system. Med. Hypotheses 4, 15-26.

Kiernan, J.A. (1979). Hypotheses concerned with axonal regeneration in the mammalian nervous system. Biol. Rev. Cambridge Philos. Soc. 54, 155-197.

Kuhlengel, K.R., Bunge, M.B., Bunge, R.P., and Burton, H. (1990). Implantation of cultured sensory neurons and Schwann cells into lesioned neonatal rat spinal cord. II. Implant characteristics and examination of corticospinal tract growth. J. Comp. Neurol. 293, 74-91.

Lampert, P., and Cressman, M. (1964). Axonal regeneration in the dorsal columns of the spinal cord of adult rats. Lab. Invest. 13, 825-839.

Landau, B.R., and Dawe, A.R. (1958). Respiration in the hibernation of the 13-lined ground squirrel. Am. J. Physiol. 194, 75-82.

Latov, N., Nilaver, G., Zimmerman, E.A., Johnson, W.G.,Silverman, A.J., Defendini, R., and Cote, L. (1979). Fibrillary astrocytes proliferate in response to brain injury. Dev. Biol. 72, 381-384.

Lieberman, A.R. (1971). The axon reaction: a review of the principal features of perikaryal response to axon injury. Int. Rev. Neurobiol. 14, 49-124.

Lieberman, A.R. (1974). Some factors affecting retrograde neuronal response to axonal lesions. In: Essays on the nervous system, (R. Bellairs and E.G. Gray eds.), pp. 71-105, Clarendon Press, Oxford.

Liesi. P., Dahl, D., and Vaheri, A. (1983). Laminin is produced by early rat astrocytes in primary culture. J. Cell Biol. 96, 920-924.

Lyman, C.P., and O'Brien, R.C. (1960). Mammalian hibernation XVIII. Circulatory changes in the thirteen-lined ground squirrel during the hibernation cycle. Bull. Comp. Zool. Harvard 124, 353-372.

Martin, D.L. (1992). Synthesis and release of neuroactive substances by glial cells. Glia 5, 81-94.

Martin, D., Schoenen, J., Delree, P., Leprince, P., Rogister, B., and Moonen, G. (1991). Grafts of syngenic cultured, adult dorsal root ganglion-derived Schwann cells to the injured spinal cord of adult rats: preliminary morphological studies. Neurosci. Lett. 124, 44-48.

Martini, R., and Schachner, M. (1988). Immunoelectron microscopic localization of neural cell adhesion molecules in regenerating adult mouse sciatic nerve. J. Cell Biol. 106, 1735-1746.

Matthews, M.A., St. Onge, M.F., Faciane, C.L., and Gelderd, J.B.

(1979). Spinal cord transection: A quantitative analysis of elements of the connective tissue matrix formed within the site of lesion following administration of piromen, cytoxan or trypsin. Neuropathol. Appl. Neurobiol. 5, 161-180.

McCarthy, K.D., and deVellis, J. (1980). Preparation of separate astroglial and oligodendroglial cell cultures from rat cerebral tissue. J. Cell Biol. 85, 890-902.

Murata, Y., Chiba, T., Brundin, P., Bjorklund, A., and Lindvall, O. (1990). Formation of synaptic graft-host connections by noradrenergic locus coeruleus neurons transplanted into the adult rat hippocampus. Exp. Neurol. 110, 258-267.

Nathaniel, E.J.H., and Nathaniel, D.R. (1973). Regeneration of dorsal root fibres into the adult rat spinal cord. Exp. Neurol. 40, 333-350.

Neugebauer, K.M., Tomaselli, K.J., Lilien, J., and Reichardt, L.F. (1988). N-cadherin, NCAM, and integrins promote retinal neurite outgrowth on astrocytes in vitro. J. Cell Biol. 107, 1177-1187.

Nornes, H., Bjorklund, A., and Stenevi, U. (1983). Reinnervation of the denervated adult spinal cord of rats by intraspinal transplants of embryonic brain stem neurons. Cell Tissue Res. 230, 15-35.

North, R.J. (1978). Concept of activated macrophage. J. Immunol. 121, 806-809.

Persohn, E., and Schachner, M. (1987). Immunoelectronmicroscopic

localization of the neural cell adhesion molecule L1 and NCAM during postnatal development of mouse cerebellum. J. Cell Biol. 105, 569-576.

Privat, A., Valat, J., and Fulcrand, J. (1981). Proliferation of neuroglial cell lines in the degenerating optic nerve of young rats. A radioautographic study. J. Neuropathol. Exp. Neurol. 40, 46-60.

Reier, P.J. (1985). Neural tissue grafts and repair of the injured spinal cord. Neuropathol. Appl. Neurobiol. 11, 81-104.

Reier, P.J., Bregman, B.S., and Wujek, J.R. (1986). Intraspinal transplantation of embryonic spinal cord tissue in neonatal and adult rats. J. Comp. Neurol. 247, 275-296.

Richardson, P.M., McGuinness, U.M., and Aguayo, A.J. (1982). Peripheral nerve autografts to the rat spinal cord: studies with axonal tracing methods. Brain Res. 237, 147-162.

Robertson, D.M., and Dinsdale, H.B. (1972). The nervous system. Structure and function in Disease. Monograph series, pp. 12-35; 141-157, Williams and Wilkins company, Baltimore.

Rudge, J.S., Manthorpe, M., and Varon, S. (1985). The output of neuronotrophic and neurite-promoting agents from rat brain astroglial cells: A microculture method for screening potential regulatory molecules. Dev. Brain Res. 19, 161-172.

Shamboul, K.M. (1979). Retrograde axon reaction in the lateral vestibular nucleus of neonatal and adult rats. J. Anat. 129, 225-233.

Sievers, J., Hausmann, B., Unsicker, K., and Berry, M. (1987). Fibroblast growth factors promote the survival of adult rat retinal ganglion cells after transection of the optic nerve. Neurosci. Lett. 76, 157-162.

Smith, G.M., and Miller, R.H. (1991). Immature type-1 astrocytes suppress glial scar formation, are motile and interact with blood vessels. Brain Res. 543, 111-122.

Strecker, R.E. (1992). Fetal transplants show promise. Science. 257, 868-870.

Torvik, A., and Heding, A. (1967). Histological studies on the effect of actinomycin D on retrograde nerve cell reaction in the facial nucleus of mice. Acta. Neuropathol. (Berl.). 9, 146-157.

Tracey, D.J. (1985). Ascending and descending pathways in the spinal cord. In: The rat nervous system, (Paxinos, G. ed.), pp. 311-324, Academic Press.

Unsicker, K., Reichert-Preibsch, H., Schmidt, R., Pettmann, B., Labourdette, G., and Sensenbrenner, M. (1987). Astroglial and fibroblast growth factors have neurotrophic functions for cultured peripheral central nervous system neurons. Proc. Natl. Acad. Sci. USA. Neurobiol. 84, 5459-5463.

Vaca, K., and Wendt, E. (1992). Divergent effects of astroglial and microglial secretions on neuron growth and survival. Exp. Neurol. 118, 62-72.

Vahlsing, H.L., and Feringa, E.R. (1980). A ventral uncrossed

corticospinal tract in the rat. Exp. Neurol. 70, 282-287.

Varon, S., and Bunge, R.P. (1978). Trophic mechanisms in the peripheral nervous system. Annu. Rev. Neurosci. 1, 327-361.

Windle, W.F. (1956). Regeneration of axons in the vertebrate central nervous system. Physiol. Rev. 36, 427-440.

Wong, L.W. (1991). Cell culture studies of olfactory receptor neurons. pp. 8-11, Master Thesis, Dept. Anatomy of The Chinese University of Hong Kong.

Zhang, F.Z. (1986). Spinal cord. In: The central nervous system of the rat Anatomical aspects, (Wang, P.Y. ed.), pp. 1-8, People's Health Publishing House (China).